11-29-2012

Projected Climate Change Impacts on the Hydrology and Temperature of Pacific Northwest Rivers

Huan Wu

John S. Kimball

Marketa M. Elsner

Nate Mantua

Robert F. Adler

See next page for additional authors

Projected climate change impacts on the hydrology and temperature of Pacific Northwest rivers

Huan Wu,[1,2] John S. Kimball,[3,4] Marketa M. Elsner,[5] Nate Mantua,[5,6] Robert F. Adler,[1,2] and Jack Stanford[3]

Received 5 March 2012; revised 10 September 2012; accepted 21 October 2012; published 29 November 2012.

[1] A dominant river-tracing-based streamflow and temperature (DRTT) model was developed by coupling stream thermal dynamics with a source-sink routing model. The DRTT model was applied using 1/16 degree (~6 km) resolution gridded daily surface meteorology inputs over a ~988,000 km^2 Pacific Northwest (PNW) domain to produce regional daily streamflow and temperature simulations from 1996 to 2005. The DRTT results showed favorable performance for simulation of daily stream temperature (mean $R^2 = 0.72$ and root-mean-square error = 2.35°C) and discharge (mean $R^2 = 0.52$ and annual relative error = 14%) against observations from 12 PNW streams. The DRTT was then applied with a macroscale hydrologic model to predict streamflow and temperature changes under historical (1980s) and future (2020s, 2040s, and 2080s) climate change scenarios (IPCC AR4) as they may affect current and future patterns of freshwater salmon habitat and associated productivity of PNW streams. The model projected a 3.5% decrease in mean annual streamflow for the 2020s and 0.6% and 5.5% increases for the 2040s and 2080s, respectively, with projected increase in mean annual stream temperatures from 0.55°C (2020s) to 1.68°C (2080s). However, summer streamflow decreased from 19.3% (2020s) to 30.3% (2080s), while mean summer stream temperatures warmed from 0.92°C to 2.10°C. The simulations indicate that projected climate change will have greater impacts on snow dominant streams, with lower summer streamflows and warmer summer stream temperature changes relative to transient and rain dominant regimes. Lower summer flows combined with warmer stream temperatures suggest a future with widespread increased summertime thermal stress for coldwater fish in the PNW region.

Citation: Wu, H., J. S. Kimball, M. M. Elsner, N. Mantua, R. F. Adler, and J. Stanford (2012), Projected climate change impacts on the hydrology and temperature of Pacific Northwest rivers, *Water Resour. Res.*, *48*, W11530, doi:10.1029/2012WR012082.

1. Introduction

[2] Streamflow and temperature are critical variables in aquatic ecosystems, casting crucial environmental constraints on habitat quantity, quality and distribution. The major influence of temperature on aquatic biota has led to renewed interest in the thermal behavior of flowing waters [*Webb et al.*, 2008]. The magnitude and temporal variability of streamflows are fundamentally linked to behavioral responses and life stages of many aquatic species [*Yang et al.*, 2005]. Water temperature is a critical determinant for organism growth, survival and distribution, influencing the metabolic rates and the timing of migration, spawning, incubation and growth of fish and other aquatic organisms [*Sullivan et al.*, 2000; *Dunham et al.*, 2003; *McCullough et al.*, 2009]. Thus, exceedance thresholds of stream temperatures represent relative metrics of potential impacts on aquatic biota [e.g., *LeBlanc et al.*, 1997; *Sullivan et al.*, 2000; *Wenger et al.*, 2011]. Warming trends have been found in observation records and model simulations for many river systems [*Webb et al.*, 2008], and warming occurs in relation to changes in timing and magnitude of stream flows [e.g., *Morrison et al.*, 2002; *Mantua et al.*, 2010]. Hereafter for simplicity we use the general term stream and streamflow to describe both streams (up to fourth order) and larger rivers, and the water flow from them.

[3] The Pacific Northwest (PNW) region of North America extends from 124°W to 111°W longitude and 41.5°N to 49.5°N latitude. The PNW domain covers ~988,000 km^2 and comprises the Columbia River basin and coastal drainages, including Washington, Oregon, Idaho, western Montana and portions of British Columbia. The hydrology of

[1]Earth System Science Interdisciplinary Center, University of Maryland, College Park, Maryland, USA.
[2]NASA Goddard Space Flight Center, Greenbelt, Maryland, USA.
[3]Flathead Lake Biological Station, University of Montana, Polson, Montana, USA.
[4]Numerical Terradynamic Simulation Group, College of Forestry and Conservation, University of Montana, Missoula, Montana, USA.
[5]Climate Impacts Group, Joint Institute for the Study of the Atmosphere and Ocean, University of Washington, Seattle, Washington, USA.
[6]School of Aquatic and Fisheries Sciences, University of Washington, Seattle, Washington, USA.

Corresponding author: H. Wu, Earth System Science Interdisciplinary Center, University of Maryland, 5825 University Ct., Ste. 4001, College Park, MD 20704-3823, USA. (huanwu@umd.edu)

0043-1397/12/2012WR012082

PNW streams is particularly sensitive to climate change because of the strong influence of winter snowpack on water supply and discharge in this largely mountainous region. Climate models used in the Intergovernmental Panel on Climate Change (IPCC) Fourth Assessment Report (AR4) point to a warming trend in the PNW over the next century; these projections include mean annual warming of 1.1°C (2.0°F) by the 2020s, 1.8°C (3.2°F) by the 2040s, and 3.0°C (5.3°F) by the 2080s, relative to historical (1970 to 1999) conditions averaged across all climate models [*Randall et al.*, 2007, *Mote and Salathé*, 2010]. Stream temperatures in some PNW and north Pacific Rim river basins are expected to increase under projected global warming scenarios [e.g., *Morrison et al.*, 2002; *Yearsley*, 2009; *Mantua et al.*, 2010]. These changes likely will have adverse impacts on PNW aquatic ecosystems including the availability, quality, distribution and abundance of freshwater habitats, notably for anadromous salmonids [*Morrison et al.*, 2002; *Beechie et al.*, 2012]. However, available simulations and projections of flow and temperature changes are constrained to streams in limited areas, with uncertain accuracy levels for the full range of PNW streams and particularly for headwaters [e.g., *Yearsley*, 2009; *Isaak et al.*, 2010].

[4] New quantitative tools are needed for improved simulations of daily streamflows and temperatures over large regions extending from headwater streams to basin outlets, and representing current and projected future climate conditions. Various model approaches have been developed to derive stream temperature from meteorological and hydrological variables, including physically based models [e.g., *Sinokrot and Stefan*, 1993; *LeBlanc et al.*, 1997; *Haag and Luce*, 2008; *Yearsley*, 2009] and empirical approaches [e.g., *Mohseni et al.*, 1998; *Mohseni and Stefan*, 1999; *Bogan et al.*, 2003; *van Vliet et al.*, 2011]. Empirical regression approaches are comparatively simple and less data intensive in relation to physically based models. However, empirical approaches do not imply causation and have limitations in their transferability outside the range of conditions from which they were developed [*Johnson*, 2003; *Ducharne*, 2007]. This limits their utility for regional applications, which may contain many basins with varying landscape and climate characteristics. Physically based models attempt to represent the major mass and energy exchange processes within stream reaches and are expected to enable relatively accurate streamflow and temperature simulations over larger regions, including entire basin stream networks. Physically based models are generally more data intensive than empirical approaches, though recent advances in availability, resolution and accuracy of meteorological forcing variables and ancillary vegetation and stream hydrography data sets enable physically based modeling of streamflow and temperatures over large spatial regions with potentially improved accuracy [e.g., *Wu et al.*, 2011; *Elsner et al.*, 2010; H. Li et al., A physically based runoff routing model for land surface and Earthsystem models, submitted to *Journal of Hydrometeorology*, 2012, hereinafter referred to as Li et al., submitted manuscript].

[5] Although streamflow and temperature conditions at the river mouth are important measures of mass and heat fluxes to the ocean [*Yang et al.*, 2005], salmon and other migratory aquatic species often are strongly influenced by flow and temperature conditions throughout the entire stream network, including small headwater streams. Large spatial and temporal variations in streamflow and temperature may naturally characterize many streams [e.g., *Marsh and Prowse*, 1987; *Poff and Ward*, 1989; *Webb and Zhang*, 1997; *Yang et al.*, 2005]. Stream temperature usually covaries with streamflow especially in temperate regions [e.g., *Constantz*, 1998; *Gu and Li*, 2002]; reduced thermal capacity occurs as flow decreases, causing increased aquatic temperature variation in relation to changes in ambient air temperatures.

[6] Dynamic hydraulic flow and heat transfer models have been effectively applied to predict stream temperature [*Sinokrot and Stefan*, 1993; *LeBlanc et al.*, 1997; *Sullivan and Rounds*, 2004]. However, previous stream temperature studies have mainly addressed specific reaches or smaller, nested subbasins at relatively fine temporal and spatial resolution. The application of these models over larger regions is uncertain, but may potentially be accomplished by networking a series of reaches [*LeBlanc et al.*, 1997]. In any case, dynamic process level approaches for deriving more extensive streamflow and temperature simulations for each grid cell within larger basins and regional domains are lacking. Additionally, few studies have examined spatial and temporal patterns of interactions between stream temperature and streamflow over large regions like the PNW.

[7] For a stream reach or segment, streamflow and temperature conditions at an upstream confluence with a tributary often represent initial boundary conditions. However, neglecting flow and temperature conditions upstream of the initial boundary can be the largest potential error source in stream temperature estimation [*Bogan et al.*, 2004]. Boundary conditions have been estimated using streamflow and temperature information from stream gauge observations or using preprocessed distributed tributary inflow data from a hydrologic model [e.g., *Sinokrot and Stefan*, 1993; *Yearsley*, 2009; *Risley et al.*, 2010]. Accurate prediction of stream temperature variation along a flow path through a stream network requires consideration of both local energy balance and the advected heat flux from upstream reaches and tributaries. Moreover, accurate discharge estimates are a prerequisite for accurate stream temperature simulations [*Gu and Li*, 2002; *Haag and Luce*, 2008]. Unfortunately, discharge and temperature observations from stream gauge networks are often sparsely distributed within large basins or regions. Nonetheless, a robust, distributed hydrologic model can supply the necessary inputs for flow and temperature estimation throughout the network, including flow magnitude and velocity, water depth and stream confluence points.

[8] Previous studies have largely focused on estimating summer stream temperatures [e.g., *Morrison et al.*, 2002; *Tague et al.*, 2007], while relatively few studies have involved continuous daily stream temperature simulations over longer periods (e.g., 1 year or longer), particularly for regional applications. Streamflow and temperature conditions for all seasons are important to ecosystem processes and should be represented by multiyear and continuous stream temperature modeling [*Morrison et al.*, 2002; *Yearsley*, 2009].

[9] The objectives of this paper are (1) to present a new coupled streamflow and temperature process model for estimating dynamic daily flow and temperature conditions along entire flow paths of regional drainage networks over

long time series and (2) to apply the streamflow and temperature model using daily runoff inputs from a macroscale hydrology model to determine historical and potential future flow and temperature conditions under projected climate change scenarios (predicted by 20 GCMs) for the PNW domain. The following sections describe the model algorithms, methods, and data used in this study. The model results are verified using available site observations within the PNW domain. Model-projected changes in simulated streamflow and temperature conditions are presented for future climate change scenarios, followed by a discussion of the environmental implications of these changes for PNW salmon populations.

2. Methodology

[10] Dynamic simulations of hydrologic variables including streamflow have been used to evaluate climate change impacts on regional hydrology [e.g., *Christensen and Lettenmaier*, 2007; *Maurer*, 2007; *Elsner et al.*, 2010]. These simulations employ hydrologic models driven by gridded surface meteorology inputs interpolated from regional weather stations and downscaled ensembles of projected climate conditions from global climate models (GCMs). For our work, a regional scale hydrologic simulation scheme was developed to predict daily streamflow and stream temperature conditions under historical (1980s) and future (2020s, 2040s, and 2080s) climate change scenarios across the PNW domain. The future climate scenarios were defined from ensemble GCM simulations of the IPCC AR4 [*Randall et al.*, 2007] for the A1B climate scenario (a middle of the road scenario in terms of total human emissions). The resulting model simulations were used to analyze spatial patterns and seasonal changes in historical streamflow and temperature conditions, and to estimate potential future flow and temperature changes under projected climate change scenarios.

[11] The simulation scheme consists of a two-step process involving (1) macroscale hydrologic model predictions of daily runoff from the variable infiltration capacity (VIC) model [*Liang et al.*, 1994, 1996] and (2) dynamic routing and stream temperature model simulations using VIC derived inputs. The VIC model was first employed to generate daily water flux (e.g., runoff, soil moisture) and associated forcing variables (i.e., incoming short-wave and long-wave radiation, vapor pressure and vapor pressure deficit) for the daily streamflow and temperature simulations. The VIC model and streamflow and temperature simulations are driven by daily surface meteorology inputs from historical reanalysis and spatially downscaled future forcing data [*Maurer et al.*, 2002; *Hamlet and Lettenmaier*, 2005; *Mote and Salathé*, 2010; *Elsner et al.*, 2010].

[12] We developed a source-sink hydrologic routing model to distribute VIC daily runoff estimates and predict streamflow for every grid cell along defined basin flow pathways. A coupled streamflow and temperature model was then developed by merging stream thermal dynamics simulations with the source-sink routing model. These models were established at coarse spatial resolution (i.e., 1/16 degree resolution in this study), and the horizontal advection of water and heat flux were accumulated along dominant flow paths defined from spatial upscaling of finer-scale (1 km resolution) stream network information. The coupled streamflow and temperature model for this investigation uses a hierarchical dominant river tracing (DRT) upscaling algorithm [*Wu et al.*, 2011] that defines the underlying hydrography used for the streamflow and temperature calculations. The DRT hydrography parameters are defined in a hierarchical stepwise (upstream to downstream) classification of grid cells that include flow direction, flow distance, drainage area and channel slope. These parameters are defined at the relatively coarse spatial resolution of the VIC model simulations from finer-scale digital terrain information. To derive coarser resolution hydrography parameters, the DRT algorithm preserves the baseline fine-scale hierarchical drainage structure by tracing each entire flow path from headwater to river mouth at fine scale while prioritizing successively higher-order basins and rivers for tracing [*Wu et al.*, 2011]. Hereafter, the hierarchical dominant river tracing based streamflow and temperature model for this investigation is referred to as DRTT. The DRTT model describes heat and water advection-dispersion processes along the DRT-defined hydrologic drainage network, starting with upstream source area cells that feed basin outlet/sink cells. Thus the model determines both streamflow and temperature on a daily basis for each point along a stream flow path. The DRTT model is described in the following sections and contains three primary modules: water and heat transport in stream networks; the coupling of hydrologic routing processes and thermal dynamics, and airshed and stream-riparian thermal dynamics.

2.1. DRTT Coupled Streamflow and Temperature Modeling

2.1.1. Streamflow and Heat Transport

[13] For all grid cells in a study domain, all upstream source area cells and associated flow paths are first identified by the DRTT model according to the DRT defined flow direction map. A grid cell to be modeled for streamflow and temperature is hereafter referred to as the target cell. The unsteady open channel streamflow without lateral flow, is described using a one-dimensional advection-dispersion equation for each cell along the flow path from a source grid cell (with runoff generated) to the target cell according to

$$\frac{\partial q}{\partial t} + c\frac{\partial q}{\partial x} - d\frac{\partial^2 q}{\partial x^2} = 0 \tag{1}$$

where q is the streamflow rate ($m^3\ s^{-1}$), c is the kinematic wave celerity ($m\ s^{-1}$), d is the longitudinal dispersion coefficient ($m^2\ s^{-1}$), t is the time (s), and x is the flow distance (m). The in-stream heat transport takes the form

$$\frac{\partial T_w}{\partial t} + c\frac{\partial T_w}{\partial x} - d\frac{\partial^2 T_w}{\partial x^2} = \frac{\Delta H \times f_A}{C_p \times M} \tag{2}$$

where T_w is the water temperature (°C), ΔH is the net heat change rate ($W\ m^{-2}$), f_A is the effective water pulse surface area exposed to the air for heat interaction (m^2), C_p is the specific heat of water ($J\ kg^{-1}\ °C^{-1}$), and M is the mass of the water pulse (kg). The effects of lakes and impoundments, groundwater interactions and canopy effects are not

represented in the DRTT model. All water particles in a water pulse are assumed to reach the sink cell in the same time interval independently. By also neglecting the dispersion term in equation (2), the rate of stream temperature change in the water pulse can be expressed as

$$\frac{\partial T_w}{\partial t} = \frac{\Delta H \times f_A}{C_p \times M} \tag{3}$$

The calculation of net heat change rate (ΔH) is described in section 2.2.

2.1.2. Coupled Streamflow and Temperature Simulation

[14] Owing to the unidirectional flow of streams, stream temperature in a target grid cell is determined from the integrated effects of the water thermal dynamics of all upstream runoff after traveling from the source grid cell(s) and along the connecting flow path to the specified target cell. Therefore, besides thermal variables, flow-related variables (e.g. volume, residence time and area of surface exposure) are also important for determining stream temperature. Upstream flow effects on stream temperature are particularly important for deriving distributed stream temperature estimates over large basins. In regional applications, nonuniform streamflows move through hierarchical stream systems where lower order tributaries with different stream temperatures merge at various confluences, resulting in large changes in associated stream temperatures that then define initial conditions for downstream reaches. Hydrologic and thermal characteristics vary spatially across larger basins. Basin hydrologic response characteristics, including runoff regime, discharge rate/amount and water residence time, must be effectively represented in a physically based distributed stream temperature model as a prerequisite for accurate streamflow and temperature simulations. Streamflow and temperature simulations can be coupled by combining the numeric solution of the one-dimensional advection-dispersion equations (equations (1) and (2)). Statistical distribution curves are widely used to define the hydrologic response function (i.e. unit hydrograph) by considering the lag time variation of water particles from different sub-grid areas. In this study, the DRTT model routing scheme uses the first-passage time probability density function:

$$\mu_i(t) = \frac{1}{2t\sqrt{\pi(t/T_i)/\Pi_i}} \exp\left\{-\frac{[1-(t/T_i)]^2}{4(t/T_i)/\Pi_i}\right\} \tag{4}$$

following *Olivera and Maidment* [1999] and *Olivera et al.* [2000] to approximate the numeric solution of the advection-dispersion equation (1), where $\mu_i(t)$ (s^{-1}) is the response function at source cell i, T_i is the average lag time (s), Π_i is a representative Péclet number (dimensionless) for the flow path from the source cell i to the corresponding sink cell (target cell). Following *Olivera and Maidment* [1999], T_i and Π_i are calculated as

$$T_i = \sum_{i=1}^{n} \frac{1}{v_i} l_i \tag{5}$$

$$\prod_i = \left[\sum_{i=1}^{n} \frac{1}{v_i} l_i\right]^2 \Big/ \sum_{i=1}^{n} \frac{d_i}{v_i^3} l_i \tag{6}$$

where v_i is the mean flow velocity (m s^{-1}), l_i is the flow distance (m), and n is the number of grid cells along the flow path. The contribution of runoff generated in each upstream source cell to the streamflow in a target cell is delineated by

$$Q(x,t) = \int_0^t U(t-s)R(x,s)ds \tag{7}$$

where $Q(x,t)$ is the routed runoff (m^3) contributed by an upstream source cell, $R(x,s)$ is the runoff generated in the source cell (m^3), and $U(t-s)$ is the hydrologic response function (dimensionless) for the source cell, defined by equation (4). The contribution of all upstream source cells to streamflow in the target cell is given by

$$Q_n(x,t) = \sum_{i=1}^{i=n} \int_0^t U_i(t-s)R_i(x,s)ds \tag{8}$$

where $Q_n(x,t)$ is the total streamflow routed to the target cell from all upstream source cells, and n is the number of upstream source cells. Based on the hydrologic response function (equation (4)), the runoff generated at each time step (R_i) within a source cell is divided into a number discrete of water pulses (p_i) (Figure 1a). A water pulse is defined as the collection of all water particles that are from the same source cell and reach the sink (target) cell at the same time step. Because it is challenging to determine the extent of the upstream zone of influence for stream temperature [*Johnson*, 2003], the DRTT model couples the streamflow and temperature simulation by tracing each water pulse beginning from the upstream source cell(s) to the target cell along the DRT defined flow path [*Wu et al.*, 2011], while applying the thermal dynamics equations on each cell (stream segment) in the flow path using local hydrologic and meteorological conditions as model drivers (Figure 1a). The temperature change of the water pulse at each time step in each stream segment along the flow path is calculated using equations for stream thermal dynamics described in section 2.2. With the advective heat flux from each source flow path, the stream temperature at the target cell is calculated as a mass weighted average (well mixed) temperature of all upstream water pulses routed to the target cell at each time step:

$$T_{w,n}(x,t) = \frac{Q_{n-1}(x,t) \times T_{w,n-1}(x,t) + U_n(t-s)R_n(x,s) \times T_w(x,t)}{Q_{n-1}(x,t) + U_n(t-s)R_n(x,s)} \tag{9}$$

where $T_{w,n}(x,t)$ is the stream temperature of the target cell at location x and time t when n upstream water pulses have reached and mixed, $Q_{n-1}(x,t)$ and $T_{w,n-1}(x,t)$ are the respective streamflow and temperature of the target cell when $n-1$ water pulses have reached and mixed, $U_n(t-s)R_n(x,s)$ is the nth water pulse, and $T_w(x,t)$ is the temperature of the nth water pulse when it reaches the target cell at time t. At any time t, the water pulses reaching the target cell may originate from any upstream portion of the basin, and some upstream source cells may contribute multiple water pulses to the target cell given runoff generated at different time steps. Each water

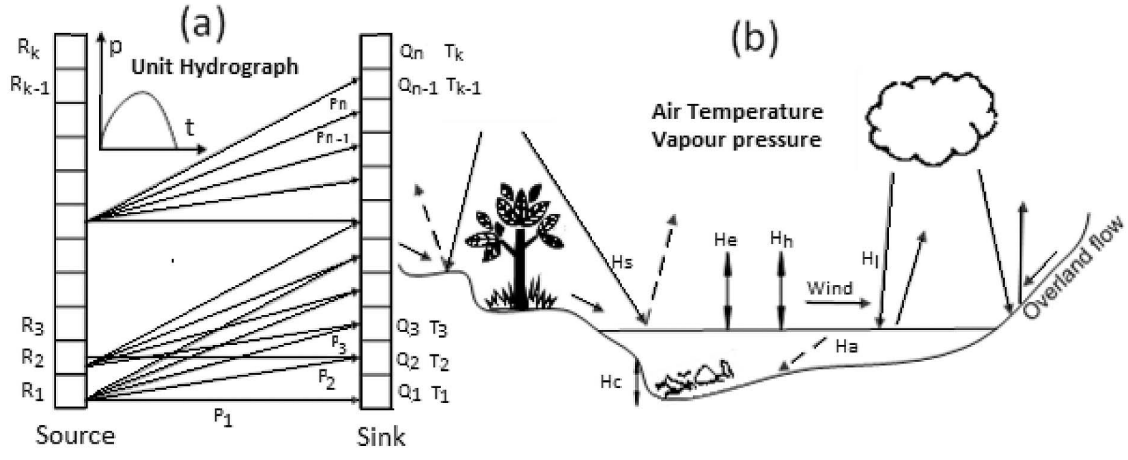

Figure 1. (a) The DRTT model couples streamflow and temperature simulation by applying thermal dynamics on each water pulse starting from a source cell to the sink or target cell. Each water pulse (P_i) comes from the total runoff (R_i) generated in a source cell at each time interval according to the unit hydrograph. The streamflow (Q_i) and temperature (T_i) of a target cell at a specific time are the sum of the discharge and average temperature from all the upstream pulses. (b) Schematic of heat fluxes (H terms; see text) at a local river reach.

pulse flows from a headwater grid cell downstream along the flow path defined by the DRT upscaling algorithm [*Wu et al.*, 2011]. Therefore, the stream temperature estimated for a target grid cell at a coarse spatial resolution (e.g., 1/16 degree used in this study) represents the bulk temperature of a vertically mixed volume of water from the dominant stream segment within the grid cell under natural conditions. The dominant stream segment is defined as the stream segment dominating the local drainage of the target cell, which also represents a segment of the larger basin stream network [*Wu et al.*, 2011]. Hereafter, the dominant stream segment is referred to as the stream reach.

2.1.3. Water Pulse Effective Surface Area

[15] Stream temperature changes in a natural stream reach are mainly controlled by thermal dynamics occurring through the water-atmosphere interface, if lateral and groundwater flows are not included. The channel water surface area is a critical variable influencing the rate of water-atmosphere heat exchange. Many factors, including flow volume and drainage density, channel morphology (particularly channel width) and shading (by vegetation and topography), can significantly affect stream temperature essentially by changing water surface area exposure to heat flux interaction. However, spatially explicit measures of these factors are largely unavailable on a regional basis. Therefore, the DRTT model employs the advection-dispersion equation (equation (2)) similar to previous studies [*Sinokrot and Stefan*, 1993; *Bogan et al.*, 2004], while using the effective surface area (f_A) of the water pulse in the heat source/sink term. For a water pulse from a source cell, the corresponding f_A at each downstream reach (cell) is estimated using a Manning type equation (10), mainly based on the water pulse volume and distance from the source cell:

$$f_A = f(x) \times \alpha \times Q_p^{\beta} \tag{10}$$

where Q_p is the magnitude of the water pulse (m^3), α and β are a dimensionless linear coefficient and exponent that define the shape of f_A response to Q_p; f_A has no effect on streamflow calculation.

[16] In upstream basin areas, kinematic waves generally dominate flow characteristics where gravity and channel bed friction are considered more important than other forces [*Chow et al.*, 1988]. Runoff tends to concentrate downstream owing to accumulation of overland flows and contributions from lower-order stream channels. For runoff routing at coarser spatial resolutions, only a single dominant river is assigned for each grid cell. However, in reality there may be many subgrid streams (flow paths) draining water downstream from a coarse grid cell area [*Wu et al.*, 2011]; each water pulse may consist of water particles from diverse areas within a source cell, and these water particles travel downstream along many smaller stream networks (or overland flow paths) out of upstream areas (not just the source cell where runoff was generated; Figure 2a). Therefore, f_A decreases along the downstream flow path when water particles tend to be constrained in a single, larger stream (Figures 2a and 2b). An additional coefficient $f(x)$ is introduced to account for the decrease in f_A along the downstream flow path as

$$f(x) = 0.8^{L/\bar{l}} \tag{11}$$

where L is the upstream dominant stream length (m) and $\bar{l}$ is the average flow distance of each grid cell from all upstream grid cells. The entire PNW domain is identified as a Strahler seventh-order river system from the DRT derived stream network at 1/16 degree resolution. In this study, once a water pulse enters a stream reach with upstream drainage area greater than 15,000 km^2 (~400 grid cells, or fourth- to fifth-order dominant stream reach at 1/16 degree resolution), the f_A term remains constant for downstream, higher-order stream reaches. The empirical shape parameters (α and β) that define the f_A response to water pulse volume Q_p (equation (10)) are determined by calibrating regional stream temperature estimates against available gauge measurements.

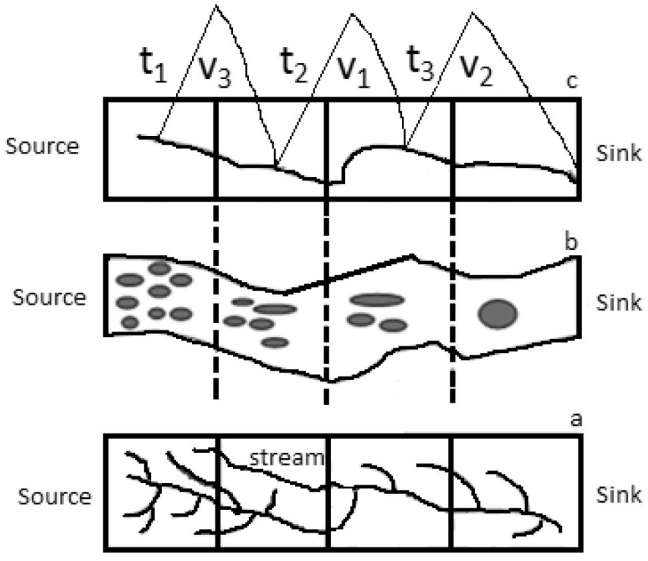

Figure 2. Schematic for a water pulse traveling through a flow path from source to sink (target) cells. (a) Each water pulse consists of water particles from the upstream source cells, including tributaries and overland flows to the sink cell downstream. (b) The effective surface area of a water pulse decreases along the downstream flow path. (c) The water pulse lag time (t_i) and flow velocity (v_i) are estimated for each stream reach along the main stem of the flow path as defined from the fine-scale hydrography data.

Calibration of α and β can partially compensate for potential reductions in model temperature accuracy due to unavailability of ancillary information on stream shading, flow path density and distance to headwater, and limited knowledge of their effects on f_A along streamflow paths. Calibration of the α and β parameters, and resulting effective water pulse surface area is a model simplification that decreases DRTT requirements for additional process information influencing f_A along river flow paths. Model performance sensitivity in response to α and β is discussed in section 6.

2.1.4. Exposure Time at Each Stream Reach

[17] The thermal advection-dispersion equation (2) is applied to each water pulse in each grid cell along a stream flow path from source cell to target cell. The exposure time (i.e., lag time) in each stream reach is important for determining the amount of water pulse heat gain and loss. The lag time is also important, especially for larger streams or longer flow paths, for determining the time and duration of local meteorological forcings described in section 2.2. The water pulse lag time (t_i) is estimated for each stream reach according to the estimated flow distance (l_i) and flow velocity (v_i) (Figure 2c):

$$t_i = \frac{l_i}{v_i} \tag{12}$$

Flow distance is obtained from the DRT upscaling algorithm [*Wu et al.*, 2011]. The DRT hydrography for this study was obtained from the 1 km resolution HYDRO1K global database (Earth Resources Observation and Science Center, USGS, http://eros.usgs.gov/#/Find_Data/Products_and_Data_Available/gtopo30/hydro). A spatially distributed but time-invariant flow velocity field was estimated using the HYDRO1K hydrography according to the method proposed by *Maidment et al.* [1996], which employs upstream drainage area in Manning's equation to allow flow velocity to increase downstream where water tends to deepen with larger upstream drainage area, and effective resistance of the river channel on flow diminishes because of larger hydraulic radius. The velocity field is also used for deriving the hydrologic response function (equation (4)).

2.1.5. Headwater Temperature

[18] It is very challenging to explicitly model the physical processes to estimate headwater (source cell) temperature from the beginning of precipitation to the time when runoff reaches a headwater stream, due to a paucity of supporting physical data over larger basins. Identification of headwater streams over large basins also remains an open challenge. For a specified headwater cell, we use a single water temperature for all runoff entering a headwater stream, which defines the DRTT temperature model initial condition; the initial water temperature at the source cells is hereafter referred to as the headwater temperature. For mesoscale or macroscale stream water temperature analysis, the influence of headwater temperature on downstream water temperature rapidly diminishes through active heat exchange across the air-water interface along river flow paths [*Mohseni and Stefan*, 1999; *Haag and Luce*, 2008; *Yearsley*, 2009]. Therefore, we estimate the headwater temperature ($T_{headwater}$) as a simple linear function of mean annual air temperature (T_{annual}) and actual air temperature (T_{air}) of the overlying grid cell (equation (13)). T_{annual} is assumed to approximate groundwater or mean annual runoff temperature and the steady component of headwater temperature, while T_{air} represents the influence of short-term air temperature variability on headwater temperatures. T_{annual} can also indicate, to some degree, the impacts of different characteristic runoff regimes (e.g., cool snowmelt runoff versus warmer rainfall-runoff) on headwater temperature. This approach is a simplification of complex processes, but has been shown to produce reasonably accurate headwater conditions for macroscale simulation of stream water temperatures [*Haag and Luce*, 2008].

$$T_{headwater} = \min\left\{\begin{array}{l} \max\left\{\begin{array}{l} T_{annual} + 0.3 * (T_{air} - T_{annual}) \\ 0.0 \end{array}\right\} \\ if\,(T_{headwater} > 12.0) \\ 12.0 + 0.5 * (T_{air} - 12.0) \end{array}\right\} \tag{13}$$

2.2. Stream Thermal Dynamics

[19] The DRTT model defines the energy balance for each water pulse and time step by estimating corresponding radiation, evaporation, conduction, convection and advection components. Stream temperature change occurring during the water pulse transit period through a specific stream reach is determined by the stream thermal dynamics as determined from six energy or heat (H) source and sink terms (Figure 1b). Thus the change in reach-specific net heat balance (ΔH) is determined as the sum of component energy gains and losses at each time step:

$$\Delta H = H_s + H_l + H_e + H_c + H_h + H_a \tag{14}$$

where H_s and H_l are net solar short-wave and long-wave radiation (W m^{-2}), H_e is the flux of latent heat (W m^{-2}), H_c is the conductive heat flux (W m^{-2}) at the streambed, H_h is the flux of sensible heat (W m^{-2}), and H_a is the advective heat flux (W m^{-2}). H_s is the difference between incoming and reflected short-wave solar radiation (H_{si}), with the reflected solar radiation (albedo) estimated as 3% of H_{si} [*Caissie et al.*, 2007; *Hebert et al.*, 2011]. The H_l term is estimated as the difference between incoming atmosphere long-wave radiation (H_{li}) and long-wave radiation emitted by the water (H_{lw}):

$$H_{lw} = 0.97 \times \sigma \times (T_w + 273.15)^4 \tag{15}$$

where 0.97 represents the water emissivity for long-wave radiation [*Anderson*, 1954], σ is the Stefan-Boltzmann constant (5.67×10^{-8} W m^{-2} K^{-4}). The H_{si} and H_{li} terms are calculated from the VIC model based on local daily air temperature maxima and minima, and precipitation following *Kimball et al.* [1997], *Thornton and Running* [1999], and *Bras* [1990]. The H_e term is estimated as

$$H_e = -\rho \times E \times Le/(86.40 \times 10^6) \tag{16}$$

where ρ is the water density (kg m^{-3}), E is the evaporation rate (mm d^{-1}), Le is the latent heat of vaporization (J kg^{-1}), and 86.40×10^6 converts units from mm d^{-1} to m s^{-1}. The evaporation rate is determined as

$$E = K_l \times (e_{sat} - e) \tag{17}$$

where K_l is an empirical coefficient for the turbulent exchange of water vapor (mm/(d hPa)), e_{sat} is the saturation vapor pressure at the water surface (hPa), and e is the actual vapor pressure (hPa). The e_{sat} and e terms are also estimated from the VIC model following *Kimball et al.* [1997] and *Thornton and Running* [1999]. The K_l term is defined as

$$K_l = 0.211 + 0.103 \times V_{wind} \times F_{wind} \tag{18}$$

where V_{wind} is the estimated local wind speed (m s^{-1}) at 10 m height, F_{wind} is a dimensionless factor for wind sheltering by riparian vegetation. L is estimated from T_w by the Magnus-Tetons formula:

$$Le = 2499.64 - 2.51 \times T_w \tag{19}$$

The H_h term is estimated from *Haag and Luce* [2008] as

$$H_h = -\gamma \times \frac{P}{1013} \times K_l \times Le \times \frac{T_w - T_{air}}{86.40 \times 10^6} \times \rho \tag{20}$$

where γ is the psychrometric constant at normal pressure (0.655 hPa/°C), P is the actual air pressure (hPa). The conductive heat flux (H_c) is estimated as a fixed proportion (assumed 5%) of the net solar radiative flux. With all energy sources and sinks defined above, equation (3) can be further expressed as

$$\frac{T_{w,n+1} - T_{w,n}}{\Delta t} = \frac{f_A \times \left[H_s + H_l + H_e + H_c + \frac{K \times (T_{w,n+1} + T_{w,n})}{2} - K \times T_{air}\right]}{C_p \times M} \tag{21}$$

where

$$K = -\gamma \times \frac{P}{1013} \times K_l \times Le \times \rho/(86.4 \times 10^6) \tag{22}$$

Equation (21) states that the change of heat storage in each water pulse and time step is equivalent to the heat exchange between the water pulse and its surrounding environment.

3. VIC and DRTT Inputs and Outputs

[20] Both the VIC and DRTT models were run at a daily time step and 1/16 degree spatial resolution for all PNW basins. The simulations require gridded daily surface meteorology inputs as primary model forcings. These data were obtained from a database of existing PNW historical surface meteorology and projected climate change scenarios that were previously used for VIC model simulations over the PNW domain [*Elsner et al.*, 2010]. These data include a 1/16 degree resolution gridded data set of historical (1916–2006) daily precipitation and air temperature (T_{mx}, T_{mn}) derived from surface station observations following *Maurer et al.* [2002] and *Hamlet and Lettenmaier* [2005]. Daily wind speed values were downscaled from National Centers for Environmental Prediction–National Center for Atmospheric Research (NCEP-NCAR) reanalysis products [*Kalnay et al.*, 1996]. Other VIC forcing variables were derived from the daily air temperature range or mean air temperature following *Maurer et al.* [2002].

[21] The VIC and DRTT simulations of projected future (to 2100) conditions were derived using regionally downscaled daily surface meteorology inputs derived from IPCC GCM climate change scenarios [*Randall et al.*, 2007]. The data were obtained from a common set of global 21st century climate simulations archived from 21 individual GCMs driven by several greenhouse gas emissions scenarios described in the IPCC Special Report on Emissions Scenarios (SRES) [*Intergovernmental Panel on Climate Change*, 2000; *Randall et al.*, 2007]. Among all SRES scenarios, the B1, A1B and A2 scenarios were commonly chosen as GCM forcings representing respective low-, medium-, and high-emission scenarios. In this study we selected the A1B scenario based GCM future climate simulations as primary VIC and DRTT model forcings to evaluate potential climate change impacts on estimated streamflow and temperature conditions in the PNW basins. The ~3° (latitude by longitude) GCM spatial resolution is generally too coarse for hydrologic model simulations. For this investigation, we used the composite A1B emission scenario PNW regional climate change projection database from *Elsner et al.* [2010],

which used a delta method [*Hamlet and Lettenmaier*, 1999; *Loáiciga et al.*, 2000] for regional downscaling of the GCM outputs to 1/16 degree resolution. The perturbations, or deltas, were derived from 20 IPCC GCM simulations for the A1B scenario and consist of projected regional monthly mean changes in average PNW temperatures (°C) and precipitation (%) for future periods.

[22] We examined the GCM projected daily simulations for estimated average conditions for three future periods, including 2010–2039 2030–2059 and 2070–2099 following *Elsner et al.* [2010] and *Mote and Salathé* [2010]; these respective periods are hereafter denoted as the 2020s, 2040s and 2080s. For future simulations at each grid cell, the VIC model was driven by observed daily maximum and minimum air temperatures added to the distributed temperature delta value and daily precipitation multiplied by the distributed precipitation fraction delta value [*Elsner et al.*, 2010; *Mote and Salathé*, 2010]. The resulting VIC simulations were used to generate daily runoff and other forcing variables that were then used as primary drivers of the DRTT simulations. The delta method described above preserves realistic temporal sequencing associated with the historical record, avoids bias in the GCM simulations, and allows for the evaluation of climate change impacts in the context of historical events [*Elsner et al.*, 2010]. However, this approach ignores potential changes in higher statistical moments (e.g., variance, skewness) of future climate distributions relative to historical conditions [*Mote and Salathé*, 2010].

[23] The VIC model generated runoff was routed by the DRTT model using spatial hydrography data (including flow direction, flow distance, channel slope, upstream drainage area and flow velocity field) generated from the DRT stream network upscaling algorithm and HYDRO1K baseline hydrography inputs [*Wu et al.*, 2011]. The daily surface meteorology forcings required for the DRTT stream thermal dynamics simulations include incoming shortwave and long-wave solar radiation, surface atmospheric pressure and humidity, and vapor pressure deficit; these variables were generated by the VIC model running in the forcing mode. Other DRTT inputs include daily surface wind speed and mean air temperature, and were obtained from the same sources used for the VIC model wind and temperature forcings described above.

4. Model Calibration and Validation

[24] Model calibration was used to improve the performance of VIC and DRTT regional simulations. The VIC runoff simulations provide critical inputs for the DRTT model and were calibrated prior to the DRTT stream temperature calibration process. Daily stream discharge data from regional gauge observations are widely available in the PNW domain, while observations for stream temperature are comparatively sparse. Regional gauges having both streamflow and temperature observations were prioritized for model validation. In order to establish the validity of the models, the streamflow and temperature simulations were compared with available independent historical observations from 12 streams and 14 gauges (observations of either streamflow or temperature, or both) distributed across the PNW domain (Figure 3). The Nash-Sutcliffe coefficient

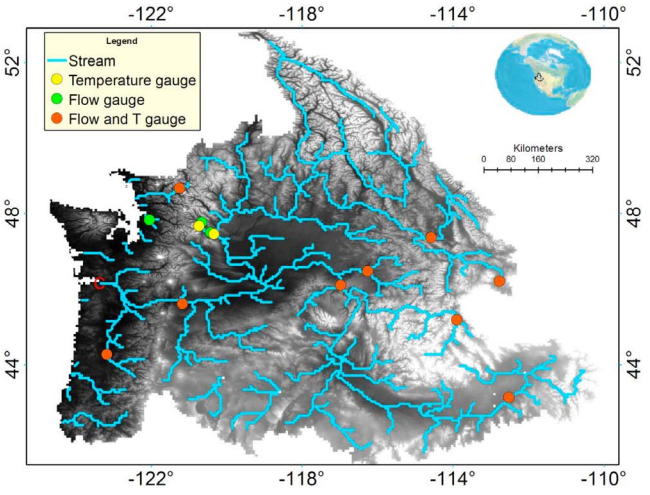

Figure 3. PNW domain and streamflow and temperature gauges. The gauges in orange have observations for both streamflow and temperature, while the gauges in green and in yellow have only streamflow and temperature observations, respectively. The blue lines are the 1/16 degree spatial resolution stream networks derived by the DRT [*Wu et al.*, 2011] using HYDROK1K hydrography data. The capital C (in red) indicates the location of the outlet of the Columbia River Basin. The gray background is the HYDRO1K DEM of the domain.

(NSC) [*Nash and Sutcliffe*, 1970], root-mean-square error (RMSE), mean absolute error (MAE), annual relative error (ARE) and correlation coefficient (R) metrics were derived from these comparisons and used to evaluate relative agreement between the simulated results and observations:

$$\mathrm{NSC} = 1.0 - \frac{\sum_{i=1}^{N}(S_i - O_i)^2}{\sum_{i=1}^{N}(O_i - \overline{O})^2} \tag{23}$$

$$\mathrm{RMSE} = \frac{1}{N}\sum_{i=1}^{N}(S_i - O_i)^2 \tag{24}$$

$$\mathrm{MAE} = \frac{1}{N}\sum_{i=1}^{N}|S_i - O_i| \tag{25}$$

where O_i is the observed streamflow or temperature; S_i is the corresponding model simulated variable; $\overline{O}$ is the average value of O_i; and N is the number of days. Daily and monthly NSC, daily R and ARE metrics were used for evaluation of the streamflow simulations, while daily and monthly NSC, daily RMSE, MAE and R metrics were used for evaluating the stream temperature simulations.

4.1. Streamflow

[25] The VIC model has been successfully used for previous hydrologic simulations and water resource management studies in the PNW [e.g., *Hamlet and Lettenmaier*, 2000;

Hamlet et al., 2010a, 2010b; *Elsner et al.*, 2010], and is generally well parameterized in this domain for water and energy balance simulations. For this study, we used the same 1/16 degree resolution gridded and calibrated soil parameters as *Hamlet et al.* [2010a] for the VIC PNW runoff simulations.

[26] Additional model calibration was performed in some subbasins (with relative less regulation) where the monthly NSC was below 0.5 or the daily NSC was below 0.1 for streamflow, and both streamflow and temperature observations were available. Model calibration was also performed for two subbasins represented by USGS stream gauge observations at Salmon River (13302500) and Clark Fork (12323800) sites; the model streamflow calculations were calibrated using five years (1996–2000) of available daily discharge records from these stations. The VIC model calibration was only performed for runoff generation because all other parameters for hydrologic routing were obtained from the DRT hydrography inputs (see section 2). The VIC runoff parameters used for calibration include the top two soil layer thicknesses (m), infiltration rate parameter (b_infilt), maximum base flowrate (Dsmax), base flowrate fraction (Ds) and fraction of bottom soil layer moisture (Ws).

[27] We calibrated the VIC model with the DRTT routing scheme using the SCE-UA method [*Duan et al.*, 1992] against daily streamflow gauge data. The SCE-UA method is based on a synthesis of deterministic and probabilistic approaches, including competitive evolution and complex shuffling techniques, making the method effective and flexible for hydrologic model calibration [*Duan et al.*, 1992, 1994]. In this study, the SCE-UA was implemented for optimizing NSC and ARE objective functions against available streamflow observations. The resulting calibrated simulations indicated improved model performance over the uncalibrated simulations in relation to the station streamflow measurement records (not shown).

[28] We validated the streamflow simulations using ten year (1996–2005) observation records from twelve USGS gauges of which nine sites included both daily discharge and temperature data (Figure 3), while three sites had only discharge data. The model validation was performed at daily and monthly scales, with validation metrics for all of the gauges presented in Table 1. Simulated and observed hydrographs for selected USGS gauge stations are also presented in Figure 4. The mean daily and monthly NSC values for all selected gauges are 0.52 and 0.70 respectively, while the mean annual relative error is 0.14 and mean

Table 1. Model Validation at Stations[a]

Gauge	Drainage Area (km^2)	NSC (d)	NSC (m)	R	ARE	RMSE	MAE
USGS 14105700, Columbia River	613,827						
Flow		0.12	0.51	0.76	0.07		
Temperature		0.18	0.88	0.82		4.28	3.02
USGS 13334300, Snake River	240,765						
Flow		0.72	0.83	0.92	0.005		
Temperature		0.87	0.90	0.94		2.36	1.46
USGS 14166000, Willamette River	8,857						
Flow		0.47	0.70	0.90	0.17		
Temperature		0.79	0.85	0.93		2.07	1.08
USGS 13069500, Snake River	29,292						
Flow		0.34	0.65	0.81	0.19		
Temperature		0.60	0.61	0.83		3.16	1.96
USGS 13302500, Salmon River	9,738						
Flow		0.64	0.71	0.90	0.21		
Temperature		0.60	0.99	0.88		2.06	1.15
USGS 12323800, Clark Fork	1,686						
Flow		0.23	0.78	0.89	0.18		
Temperature		0.89	0.94	0.95		2.04	1.08
USGS13340000, Clearwater River	14,452						
Flow		0.75	0.77	0.94	0.11		
Temperature		0.94	0.97	0.97		1.76	0.86
USGS 12462500, Wenatchee River	3,369						
Flow		0.76	0.86	0.93	0.08		
Temperature		0.73	0.87	0.86		2.18	1.24
USGS 12457000, Wenatchee River	1,530						
Flow		0.69	0.77	0.90	0.18		
Temperature		0.74		0.90		1.59	0.70
USGS 12178000, Skagit River	3,043						
Flow		<0	<0	0.29	0.12		
Temperature		0.47	0.55	0.72		1.62	0.88
USGS 12388700, Flathead River	22,778						
Flow		0.23	0.37	0.74	0.26		
Temperature		0.82	0.86	0.94		2.80	1.89
USGS 12150800, Snohomish River	3,980						
Flow		0.72	0.69	0.88	0.15		

[a]Validation metrics for streamflow are based on simulations for the 1996–2005 period, while the stream temperature metrics are based on the simulations for the 1996–2002 period. NSC(d) and NSC(m) represent daily (d) and monthly (m) summaries.

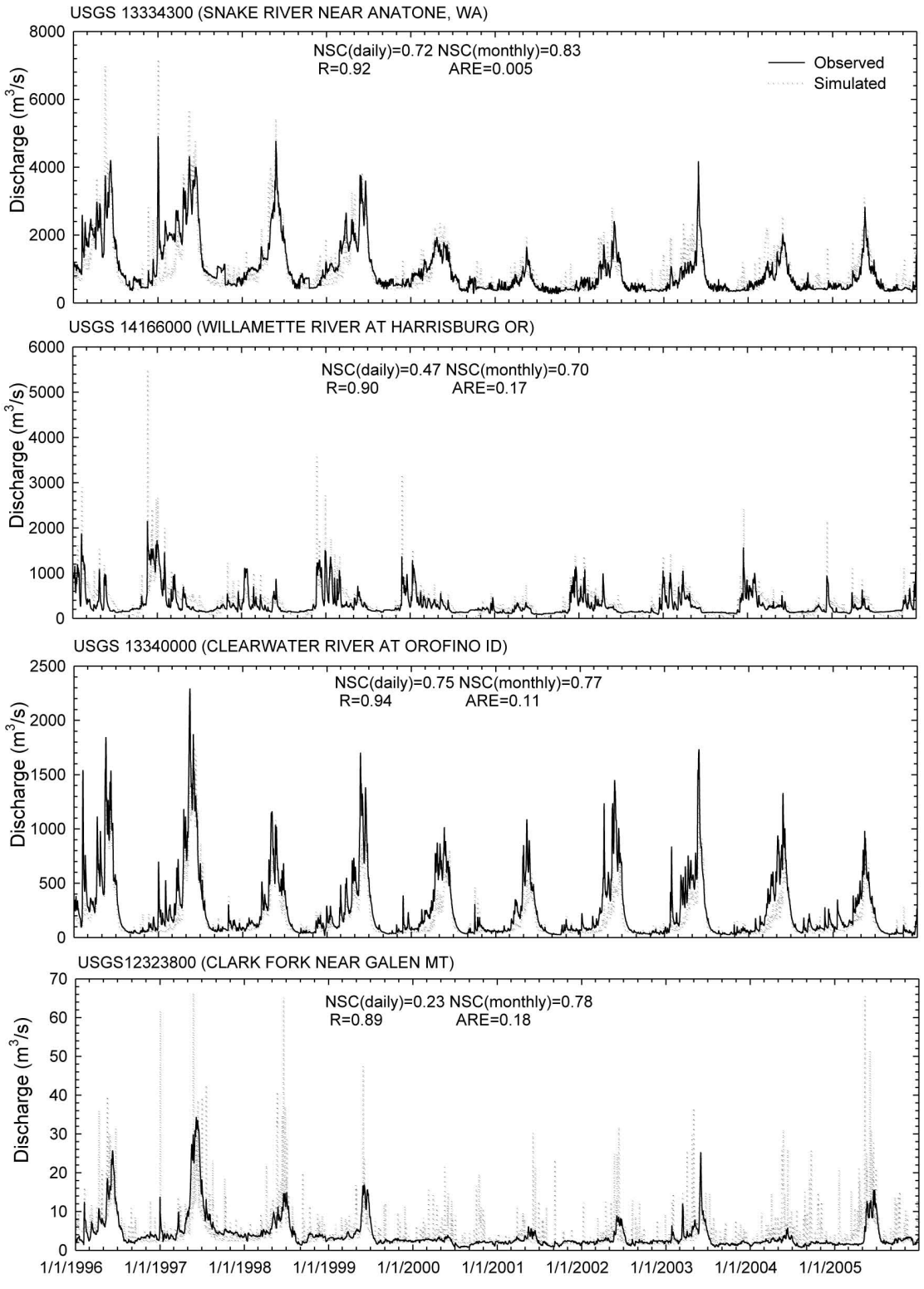

Figure 4. Comparison of predicted and measured mean daily discharge from four USGS gauges within the PNW domain.

correlation coefficient (R) is 0.82. These results indicate that the DRTT routing scheme has generally good performance at the gauge locations.

[29] The current model structure represents natural flow conditions and does not explicitly represent river regulation effects and other direct human impacts on streamflow and temperature. River regulation can adversely affect the relationship between model natural flow simulations and streamflow observations [*Elsner et al.*, 2010; Li et al., submitted manuscript], especially for the PNW domain where the river system is under extensive regulation. These effects are partially represented by the model calibration process. We evaluated the effect of river regulation on the model-gauge streamflow comparisons for a lower PNW river location (USGS 14105700) at The Dalles, OR where we compare observations, estimated naturalized flows [*Hamlet et al.*, 2010a], and model streamflow simulations. These results indicate favorable agreement (NSC = 0.85, ARE = 0.10, R = 0.96) of spatially integrated flows at this downstream PNW location and at the monthly time step against naturalized flows over a 2 year (1997–1998) record for this site. Model-data agreement is generally better against naturalized streamflow in accordance with model representation of natural flow conditions, though model performance was also favorable against the observed, unadjusted flows. These results indicate favorable performance for representing both natural and observed PNW flow conditions on a monthly basis, despite the lack of a more explicit model representation of river regulation effects. However, river regulation impacts may be larger for upstream locations closer to major impoundments and reservoirs that may not be adequately represented from the relatively sparse PNW gauge network used for model validation.

[30] Gauges representing relatively smaller upstream drainages and undeveloped areas, including Salmon (USGS 13302500), Clark Fork (USGS 12323800), and Clearwater (USGS 13340000) gauges showed generally better DRTT performance that was attributed to more natural flow conditions represented by these areas. The Skagit River site showed lower model performance relative to other validation sites (Table 1); the lower model performance reflects the influence of much stronger river regulation in the Skagit basin, where three major upstream dams (Gorge, Diablo, and Ross) provide approximately 25% of the electric power for Seattle. The anomalous spikes in the Clark Fork flow simulations (Figure 4) were mainly caused by the smaller basin drainage size (1686 km^2) for which the daily runoff-routing simulations are sensitive to daily precipitation variations.

4.2. Stream Temperature

[31] The DRTT streamflow and temperature simulations are sensitive to the effective surface area of the water pulse (f_A) and associated calibration parameters α and β (equation (10)). Based on the model calibration efforts and previous studies [e.g., *LeBlanc et al.*, 1997; *Maidment et al.*, 1996], β was set as an empirical constant (0.51), while α was calibrated between $0 \sim 100$. Despite the biological importance of stream temperature, there is a paucity of long-term water temperature observation data. The USGS may have the most intensive and continuous regional stream temperature gauge network, which is still sparse compared to a much denser PNW streamflow gauge network. The DRTT temperature model was manually calibrated (by adjusting α) against mean daily stream temperature observations at nine USGS stream temperature gauges (Figure 3) from 2003 to 2005; this period was selected for model calibration because there were relatively few gaps in the site observations relative to other years of record. These sites were also used for model validation using a different measurement period (1996∼2002). Two additional stream temperature gauges (45A070, 45A110) run by the Washington Department of Ecology (www.ecy.wa.gov/programs/eap/fw_riv/rv_main.html) were used for further independent validation of the DRTT stream temperature simulations; these sites are colocated with the USGS streamflow gauges (12462500, 12457000) used for validating model streamflow calculations (Figure 3). The main DRTT calibration strategy involved adjusting model parameters hierarchically, first within upstream basins, followed by downstream basins; once an upstream basin was calibrated, parameters were fixed and the resulting simulations used for calibrating downstream areas. The resulting temperature validation metrics are shown in Table 1 and include daily and monthly NSC, RMSE, and MAE values. Simulated and observed daily stream temperature conditions are also presented for the four selected USGS gauge sites in Figure 5.

[32] The DRTT simulations did not produce consistent overestimation or underestimation of stream temperatures over the PNW domain, though apparent model bias varies spatially because of variable stream channel environment, atmospheric conditions, and anthropogenic effects (e.g., impoundments) which may lead to warmer or cooler water temperatures, whereas the DRTT model only considers major natural flow thermal dynamics. The model calibration and validation procedure indicated that the DRTT stream temperature simulations are sensitive to the relative accuracy of VIC runoff and DRTT streamflow simulations. Overestimation (underestimation) of stream temperatures generally results from underestimation (overestimation) of streamflow. Better stream temperature accuracy tends to be achieved when the corresponding DRTT streamflow is relatively better simulated (e.g., Table 1). For example, at the Clearwater River site (USGS 13340000) both the magnitude and timing of streamflow are relatively well simulated (i.e., daily and monthly NSC values >0.70, R = 0.94, ARE = 11%); these results coincide with accurate stream temperature simulations (i.e., respective daily and monthly NSC values of 0.94 and 0.97, R = 0.97, RMSE = 1.76°C, MAE = 0.86°C). Lakes and impoundments, groundwater exchanges, and their effects on streamflows and temperature conditions are not represented in the model simulations, resulting in low model streamflow correspondence with gauge observations for the Skagit River site (USGS 12178000), especially regarding seasonal streamflow variability. The relatively poor Skagit streamflow simulation (i.e., negative NSC, R = 0.29) leads to inaccurate stream temperature simulations, with respective daily and monthly NSC values of 0.47 and 0.55, and reduced correlation (R = 0.72) with observational data (Table 1). The DRTT stream temperature RMSE (1.62°C) and MAE (0.88°C) values for the Skagit River site show favorable absolute values relative to the other validation sites, but actually indicate relatively large model bias for this cool water basin which

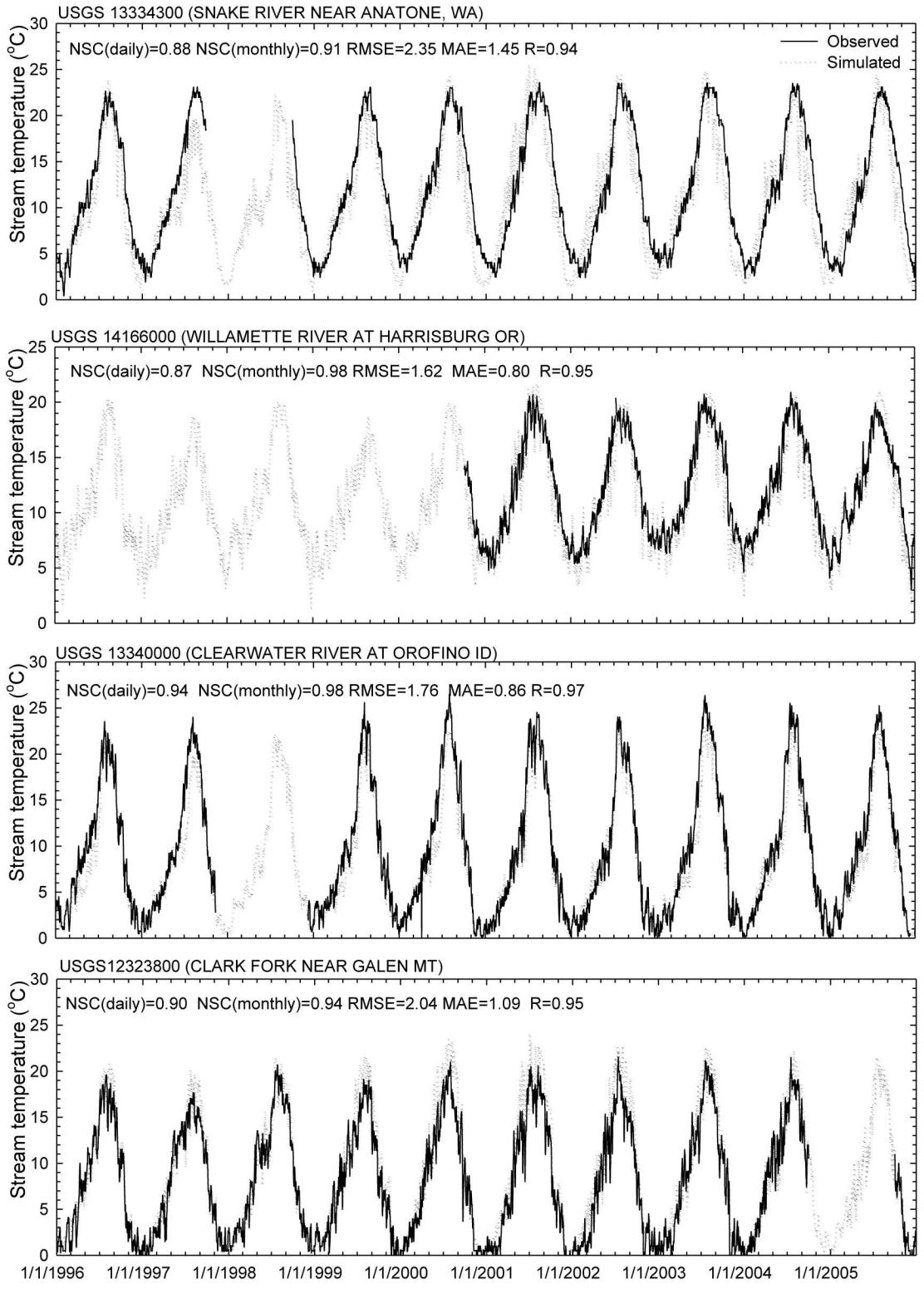

Figure 5. Comparison of predicted and measured mean daily stream temperature from four USGS gauges (same as in Figure 4) within the PNW domain.

shows a narrow mean seasonal water temperature range (~4.0°C to ~10°C). The DRTT model tends to underestimate stream temperatures along the lower Columbia stem river, which may be due to model representation of only natural stream routing and heat sources. Groundwater is less variable but is generally cooler in summer and warmer in winter compared to surface flow. In volcanic dominated PNW landscapes, including the McKenzie River catchment within the Willamette basin of western Oregon and the Deschutes River, a mid-Columbia tributary, spring flow from large and very deep (phreatic) aquifers represents a major influx of water to the stream channel and has a significant cooling effect on summer (JJA) stream temperatures [*Tague et al.*, 2007]. Extensive alluvial floodplains within the region represent areas of intensive surface-groundwater interactions that have a moderating effect on stream temperatures [*Poole and Berman*, 2001]. These processes are not represented in the regional VIC and DRTT simulations. The DRTT model without considering groundwater tends to overestimate steam temperature in summer while underestimating temperatures in the other seasons for the Willamette River station near Harrisburg OR (USGS 14166000), as shown in Figure 5. Despite these limitations, the validation results show generally favorable DRTT model performance for streamflow and temperature, including respective mean daily and monthly NSC values for temperature of 0.72 and 0.88, and favorable temperature correlations (mean R value = 0.89) and mean MAE (1.39°C) and RMSE (2.35°C) values for the 11 validation sites (Table 1).

5. Stream Temperature Model Sensitivity Analysis

[33] A DRTT performance sensitivity test was conducted for a selected PNW Salmon River observation site (USGS 13302500) for the 2004–2005 period. Model performance was first evaluated by adjusting the calibration parameter α and comparing model results against the observations. The resulting simulations showed strong sensitivity to α; the best model performance (NSC=0.70, RMSE=1.67, MAE=0.91) was achieved when the value of α is 69.7, while model performance decreases by approximately 6 to 20 percent (according to NSC) with ±10% deviations in α. The effective water pulse surface area increases in proportion to α, by which the water pulse tends to absorb/lose more heat leading to a higher/lower water temperature. β has a much narrower rational range (0.01~0.7) of variability than α, and model performance is not very sensitive to β within this range; β was therefore set as a constant (0.51) for this investigation.

[34] An additional model sensitivity test was performed to evaluate the stream temperature simulation response to air temperature and streamflow variability for the Salmon River (USGS 13302500) and 1996–2005 period by introducing respective streamflow and air temperature bias while keeping all other variables unchanged. The model stream temperature performance decreases consistently as streamflow bias increases, indicating that streamflow magnitude (water heat capacity) plays a significant role in determining stream temperature. A cool (warm) air temperature bias consistently leads to lower (higher) estimation of stream temperature. Uncertainty in either streamflow or air temperature can lead to significant bias in DRTT stream temperature simulations. A 20% streamflow decrease produced 0.56°C and 0.96°C increases in mean annual and summer stream temperature respectively, while a 2.0°C increase in air temperature produced 0.98°C and 1.25°C increases in respective mean annual and summer stream temperatures. A 20% decrease in streamflow and 2.0°C increase in air temperature produced 1.54°C and 2.21°C increases in mean annual and summer stream temperatures. These results indicate that air temperature and streamflow changes are two first-order factors that determine the model stream temperature response in a global warming context. For example, model simulations for the Salmon River (USGS 13302500) show projected 3.52°C and 7.7% increases in mean annual air temperature and streamflow by the 2080s, which results in a 2.17°C increase in estimated mean annual stream temperature. A projected 4.51°C increase in mean summer air temperature and 23.8% decrease in summer streamflow by the 2080s, leads to a 2.89°C increase in estimated mean annual stream temperature.

6. Projected Streamflow and Temperature Changes

[35] The VIC and DRTT simulations were conducted on a grid cellwise basis over the PNW domain. Both historic and future simulations used the same model setup and calibration parameters. The resulting simulations included daily streamflow and stream temperatures at 1/16 degree spatial resolution for historical (1980s) conditions and projected future climate scenarios for the 2020s, 2040s and 2080s. Regional estimates of projected climate change impacts on PNW stream flows and temperature conditions were derived by evaluating differences in model simulations of these parameters between historical and projected future conditions.

[36] The generally favorable performance of the VIC runoff and associated DRTT streamflow and temperature simulations in reproducing historical conditions represented by the available PNW observation stations, and the model sensitivity analysis provide confidence in the internal model logic and resulting predictions of future flow and temperature conditions within the domain. The same model parameters from the historical simulations were applied with the downscaled IPCC AR4 projected climate forcings to predict future streamflow and temperature conditions for the 2020s, 2040s and 2080s. Three runoff regimes were distinguished for the PNW domain, including snowmelt dominant, rain dominant, and transient systems that were characterized according to regional minimum air temperature thresholds [*Hamlet and Lettenmaier*, 2007]. In this study, we assessed projected climate change impacts on the spatial-temporal patterns of streamflow and temperature linked to regional variations in projected climate change, hydrologic characteristics and associated stream thermal dynamics across the PNW domain. Details on AR4 climate change projections for precipitation and air temperature, and associated impacts on VIC snow water equivalent (SWE), soil moisture, and runoff simulations for selected PNW basins within the three runoff regimes are given by *Elsner et al.* [2010]. Although streamflow and temperature

were calculated for each 1/16 degree grid cell over the study domain, we assessed the climate change impacts on streamflow and temperature based on stream grid cells (defined as grid cells with at least 5 contributing upstream grid cells, ~300 km^2) because regional variations in streamflow and temperature driven by relatively coarse climate change projections are less meaningful for smaller catchments [*Mote and Salathé*, 2010]. The regional assessment of climate change impacts is relatively more robust for grid cells with larger upstream drainage areas, as both streamflow and temperature for each grid cell are calculated as an integrated result of dynamic hydrologic and thermal processes of upstream grid cell drainages. Potential effects of impoundments and river regulation on stream temperature are also relatively less in higher-order streams.

[37] We assessed annual and seasonal streamflow and temperature changes by spatially averaging streamflow and temperature values from all grid cells within each runoff domain. The runoff regime for each grid cell was determined using the mean winter air temperature following *Hamlet and Lettenmaier* [2007], but using area averaged temperatures from all upstream drainage cells. The resulting snowmelt dominant runoff regime represents 48% of the PNW domain, mainly occurring on the east side of the Cascades in higher-elevation areas with lower characteristic air temperatures (Figures 6–10). The seasonal peak streamflow in these snow dominated systems generally occurs in late spring or early summer (May–July) driven by seasonal snowmelt, while low-flow conditions generally occur during the winter. Rain dominant runoff regimes represent approximately 10% of the domain and are mainly located on the west side of the Cascades at lower elevations and coastal areas with characteristic warmer air temperatures. These areas generally show seasonal peak flows in winter (December–February) and low summer flows. Transient runoff regimes represent 42% of the domain and are located throughout PNW middle elevation areas with characteristic winter air temperatures varying around freezing. These areas generally show two seasonal streamflow peaks, including a winter peak associated with seasonal precipitation and transient snow accumulation and melt events, and an additional peak in late spring or early summer associated with seasonal snowmelt. Seasonal low-flow conditions in these areas generally occur in midsummer to early fall periods.

6.1. Modeling of PNW Streamflow Changes

[38] Mean annual and summer streamflow conditions were calculated for each grid cell based on the daily DRTT model results for historical and future time periods. The predicted changes in mean annual and summer streamflows for the 2020s, 2040s and 2080s are shown in Figures 6

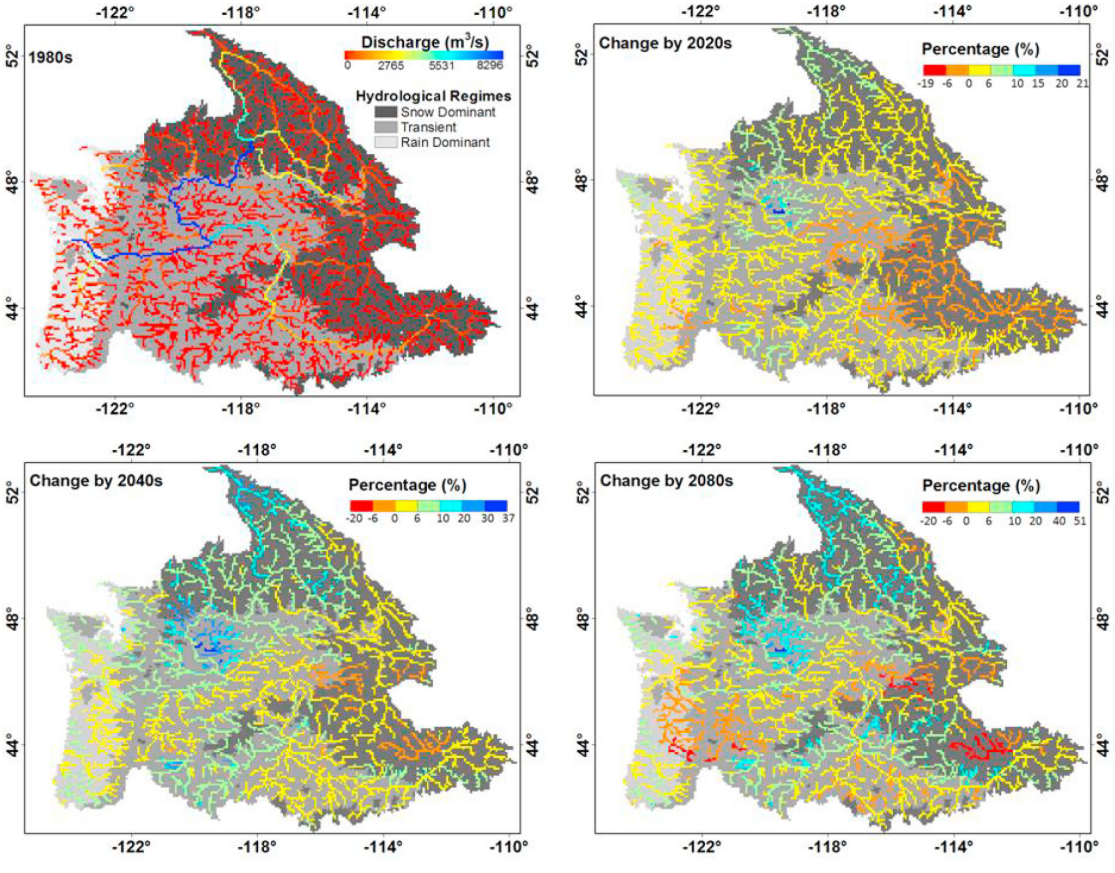

Figure 6. Projected mean annual streamflow change as compared to the 1980s over the PNW domain. The background shaded areas are the three runoff regimes: rain dominant (light gray), transient (medium gray), and snow dominant (dark gray).

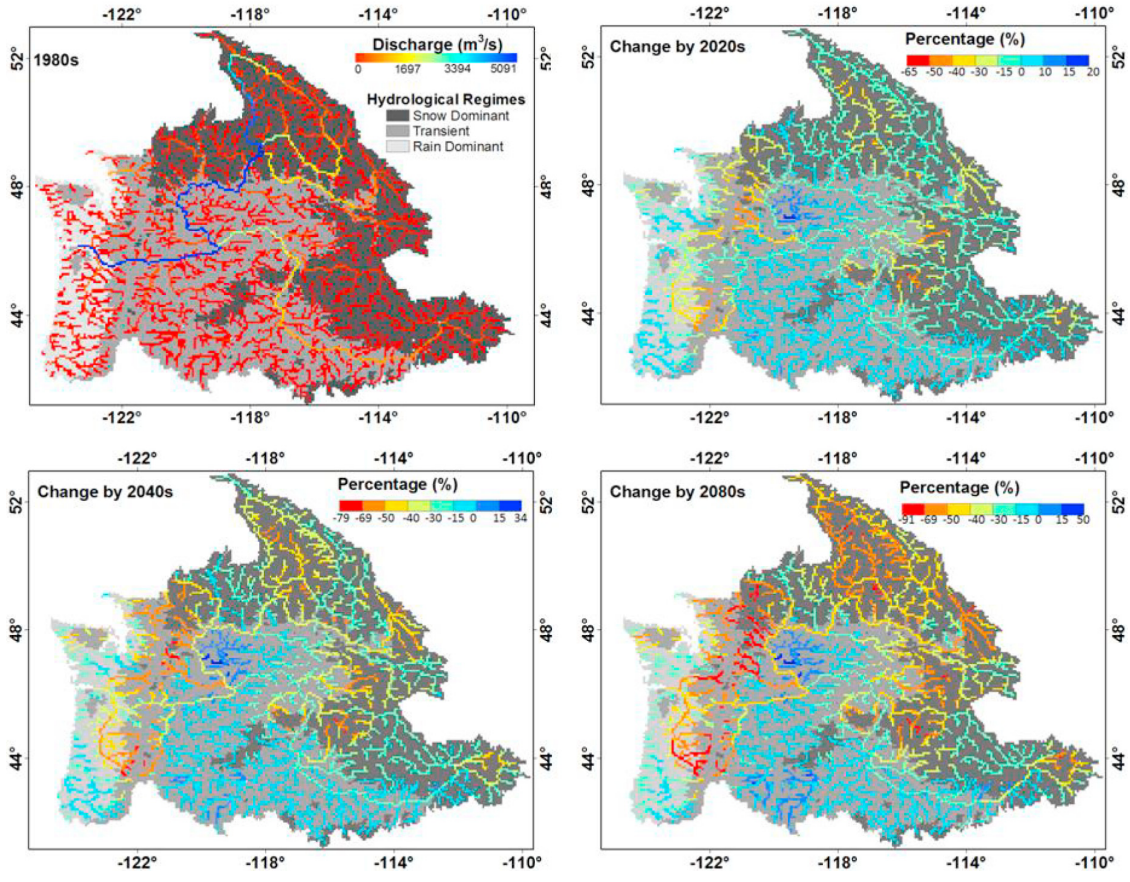

Figure 7. Same as Figure 6, but for projected mean summer streamflow change as compared to the 1980s.

and 7, respectively, as compared to the 1980s. The projected flow changes for the three PNW runoff regimes show an inconsistent trend, with reduced annual streamflow in the 2020s, but increased annual flows by the 2040s and 2080s relative to historical conditions. Average annual precipitation across the PNW is projected to increase 1.8% by the 2020s with decrease (1%) in summer and increases (2.8%) in all other seasons. However, the mean annual streamflow decreases in the 2020s are mainly driven by an average 4% increase in evapotranspiration throughout the year. In later years, the mean annual streamflow increases are mainly attributed to relatively more increase in winter precipitation [*Elsner et al.*, 2010]. Snow dominant areas show the largest projected changes ranging from a mean −4.2% (−9.1 m^3 s^{-1}) annual flow decrease by the 2020s to a mean 6.5% (34.8 m^3 s^{-1}) flow increase by the 2080s (Table 2). Areas with positive annual streamflow changes increase for all three regimes from the 2020s to 2080s. For example, positive flow trend areas in snow dominant regimes increase from 17.6% (547 cells out of 3100 cells) of the domain by the 2020s to 53.1% by the 2040s and 89.5% by the 2080s. Most of the PNW streams show a 0.6 to 5.5 percent increase in mean annual streamflow in the mid and far future periods relative to historical (1980s) conditions, with the largest (36.7 to 51.0%) projected increases occurring in the upper Columbia River basin (Figure 6). From Table 2, approximately 21% (10 out of 47) of the basin stem rivers in the PNW domain show projected increases in annual streamflow by the 2020s, while 93% (44 out of 47) of the PNW stem rivers show larger annual streamflows by the 2080s relative to historical conditions. The larger changes in magnitude and percentage are projected for annual streamflow in the far future (i.e., 2080s; Table 2).

[39] Although annual streamflow is projected to increase in most of the PNW domain by the 2040s and 2080s, summer flows decrease, with generally higher flows in the other seasons for all three runoff regimes. However, mean summer streamflow projections were more spatially variable, with increases occurring in more arid southerly and central portions of the domain (mostly in transient regime areas) and decreases occurring elsewhere (Figure 7). Although summer streamflow changes over the entire PNW domain vary greatly between −90.8∼44.8%, a negative (decreasing) flow trend is dominant over most of the domain, with 93% of all (6286) PNW stream cells showing a negative projected trend (Table 2). Projected mean summer streamflows for the PNW region show substantial decreases of 19.3%, 23.9% and 30.3% for the 2020s, 2040s and 2080s, respectively (Table 2). Summer streamflows also show relatively larger magnitude changes in the far future, with a regional mean decrease of 82 m^3 s^{-1} by the 2080s.

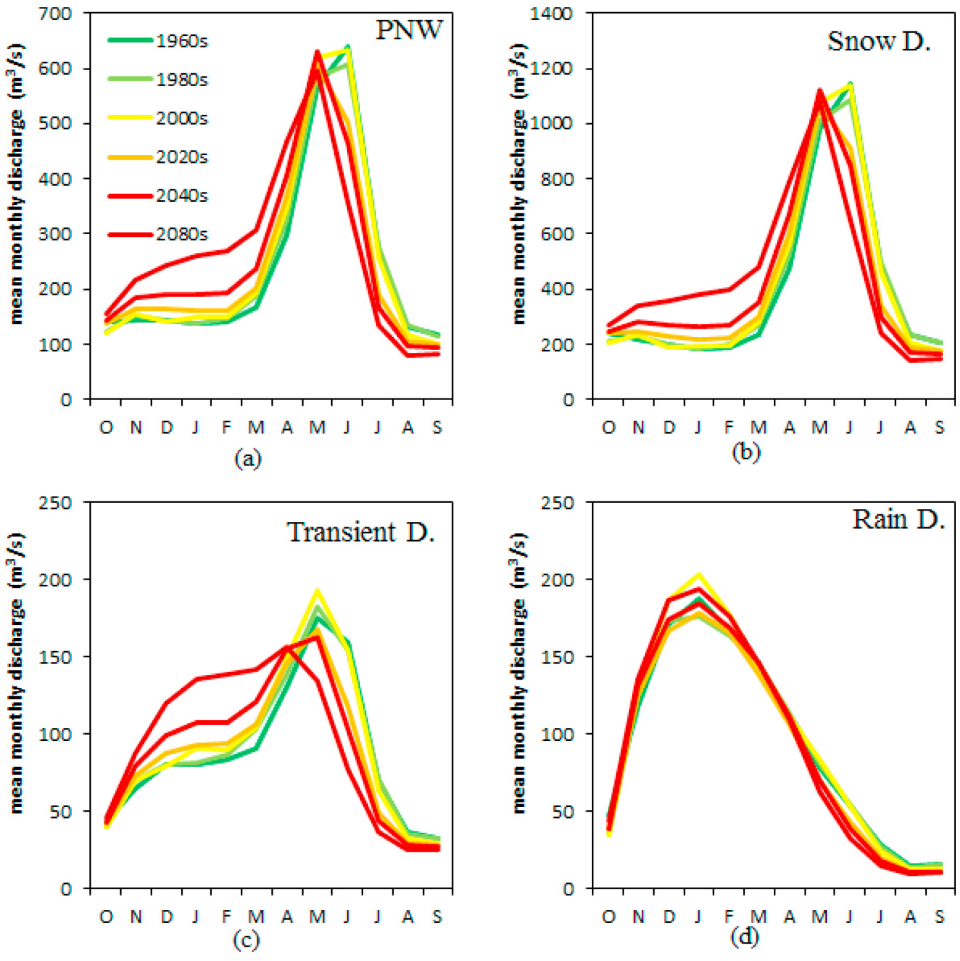

Figure 8. Hydrographs showing monthly averages of simulated daily streamflow from the VIC-DRTT model for water years for each time period, averaged across domains.

By the 2080s, the Columbia River mouth is projected to show a mean decrease of 2228.9 m^3 s^{-1} in natural summer streamflows relative to historical (1980s) conditions.

[40] Hydrographs of mean monthly simulated historical and future streamflow conditions for the three runoff regime areas and larger PNW domain are shown in Figure 8. The projected monthly streamflow changes for the three runoff regimes are similar to the projected changes in three representative watershed locations in Washington (i.e., Chehalis River at Porter, Yakima River at Parker, and Columbia River at The Dalles), described in a previous study [*Elsner et al.*, 2010]. Generally, PNW snowmelt dominant regimes (Figure 8b) are projected to shift toward more transient characteristics under a warming climate, with lower spring/early summer streamflow peaks and increased winter streamflow by the end of the 21st century. Transient regimes (Figure 8c) are projected to shift toward more rain dominant characteristics, with earlier snowmelt and associated merging of winter and spring flow peaks. Projected changes in rain dominant systems (Figure 8d) are relatively small with no clear seasonal shift in flow timing, but moderate changes in mean monthly flows. A significant (1–2 months) shift toward earlier streamflow peaks occurs for snowmelt dominant streams (Figure 8b), which is generally larger than previously reported for a single snow dominant watershed in Washington [*Elsner et al.*, 2010]. Peak flows decrease over time and occur earlier in PNW transient and snow dominant streams, which is similar to the change pattern in the nearby Fraser River (British Columbia) and a snow dominant system reported by *Morrison et al.* [2002]. The model results show significant future seasonal changes indicating a general flow increase in winter and decrease in summer relative to historical conditions. The projected average monthly hydrograph changes for the larger PNW domain (Figure 8a) are similar to the snow dominant regime results because 46% of the PNW area is classified as snowmelt dominant, with ~70% of the lower Columbia stem river water coming from the northern portion of the domain (i.e., upper Columbia River subbasin) which has a significant runoff contribution from seasonal snowmelt in mountainous headwater areas.

6.2. Modeling of Stream Temperature Changes

[41] Similar to streamflow, mean annual and summer stream temperatures were estimated from the daily stream temperature simulations for each grid cell and for each

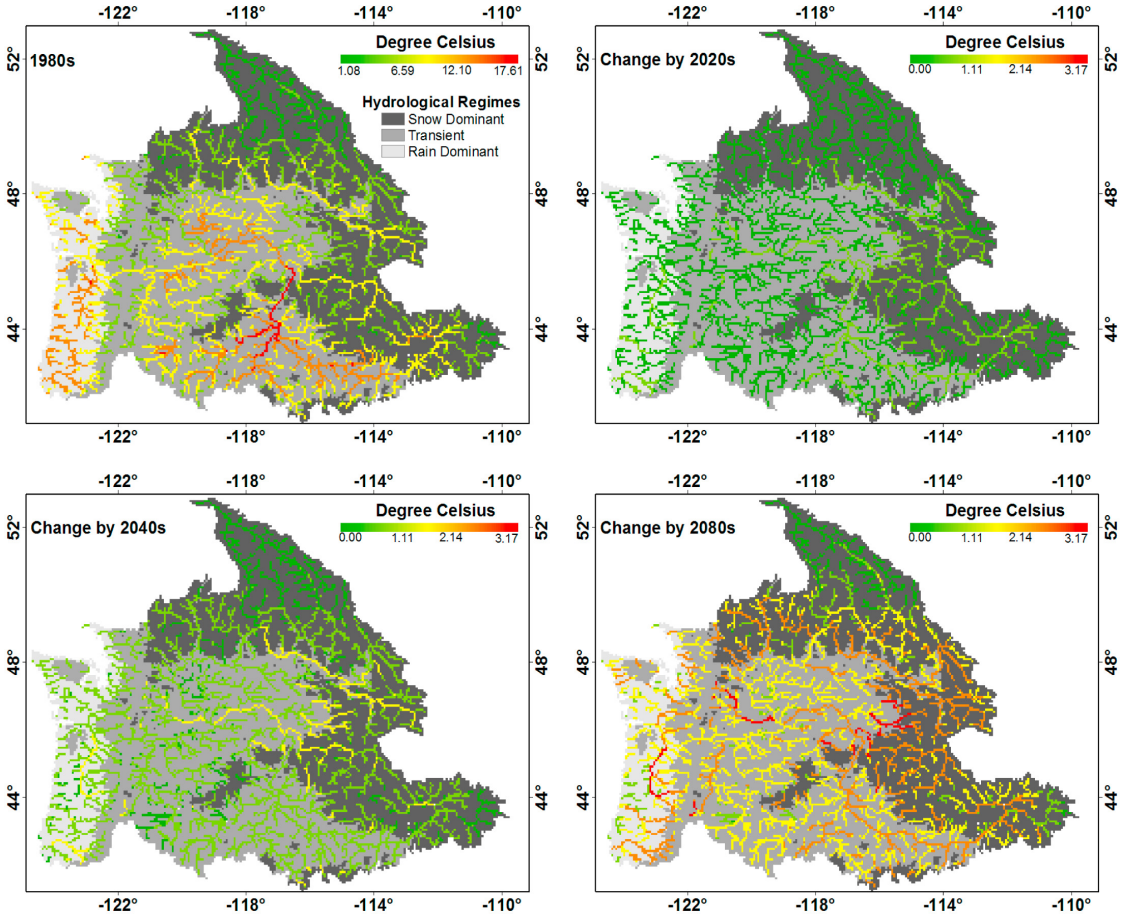

Figure 9. Same as Figure 6, but for projected mean annual stream temperature change as compared to the 1980s.

historical and future time period. The estimated changes in mean annual and summer stream temperatures for the 2020s, 2040s and 2080s are presented relative to the historical (1980s) simulations in Figures 9 and 10. The spatial patterns of changes in streamflow (Figures 6 and 7) and temperature (Figures 9 and 10) share common features. For example, projected flow and temperature changes within local stream reaches are generally similar, while abrupt spatial changes often occur at stream confluences (i.e., nodes). When a tributary with considerable flow magnitude and different temperature merges with a higher-order stream, the mixing process produces relatively abrupt downstream flow and temperature changes. These characteristics are generally consistent with observed stream temperature patterns [*Brown and Hannah*, 2008] and indicate that the model provides a realistic link between estimated stream heat budget and runoff routing processes.

[42] Almost all streams in the PNW domain show consistent projected mean annual and summer water temperature increases, but with larger summer increases relative to mean annual conditions. Mean annual stream temperatures for the PNW domain show projected increases of 0.55°C (2020s), 0.93°C (2040s), and 1.68°C (2080s) relative to the 1980s (Table 3), while mean summer stream temperatures show projected average increases of 0.92°C (2020s), 1.37°C (2040s) and 2.10°C (2080s) for the domain. The mean monthly stream temperatures averaged over the entire PNW domain and within the three runoff regimes are shown in Figure 11. Although there is no significant seasonal temperature shift, the mean monthly stream temperatures show consistent projected increases across all three runoff regimes. For the historical (1980s) period, streams are generally warmer in rain dominant and transient areas relative to snow dominant regimes (e.g., Figures 9 (top left) and 10 (top left). Snow dominant streams of the northern PNW domain (predominantly upper Columbia River basin) show generally lower projected mean annual temperature than other areas, especially the southern PNW domain (Figure 9). However, most snow dominant streams show larger projected summer temperature increases relative to estimated summer stream temperature changes in other regime areas (Figure 10). Rain dominant streams show larger projected temperature increases in winter (Figure 11), while transient streams show general projected temperature increases over all seasons.

[43] Projected air temperature changes were determined in the same way as stream temperature across the domains (Table 3). The estimated stream temperature changes are

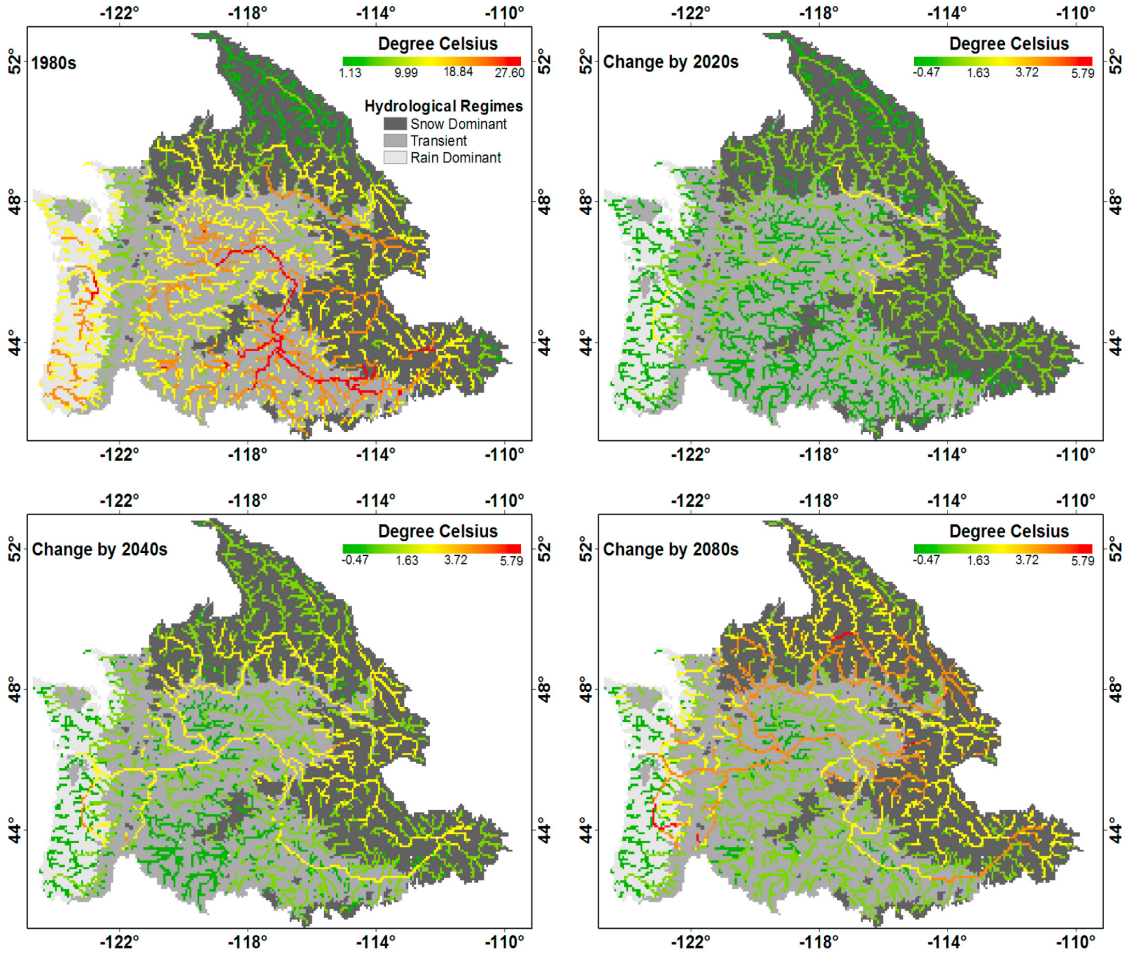

Figure 10. Same as Figure 6, but for projected mean summer stream temperature change as compared to the 1980s.

closely related to the projected air temperature and streamflow changes. The stream temperature results show consistent, but generally less warming with increasing air temperature because water has larger specific heat capacity than air and stream temperature changes are determined by the net effect of changes in streamflow and the stream energy budget. Streams with relatively lower projected temperature increases show generally strong increases in projected streamflow. This pattern is illustrated in the upper Columbia River basin, which shows large future increases in annual streamflow and only moderate warming. In contrast, streams with relatively large projected stream temperature increases coincide with large decreases in estimated future streamflow. The snow dominant streams show larger projected summer temperature increases than rainfall and transient regime streams although air temperatures for snow dominant areas are projected to have less warming than other regime areas. These results indicate that projected summer flow reductions will significantly impact summer stream temperatures in snow dominant areas. For snow dominant streams, projected warmer air temperatures result in reduced snowfall and seasonal advance in the timing of snowmelt, leading to decreased summer streamflow, which is the primary reason for relatively higher summer temperature increases in snow dominant streams. For example, estimated average summer streamflow (air temperature) decreases (increases) by 37.8% (4.46°C) for snow dominant streams, relative to respective 22.2% (4.51°C) and 27.6% (4.77°C) decreases (increases) in transient and rain dominant streams by the 2080s. Snow dominant streams show larger projected mean summer temperature increases of 1.23°C (2020s), 1.82°C (2040s) and 2.74°C (2080s) relative to transient and rain dominant regimes (Table 3). The relatively higher annual stream temperature increases projected in snow dominant streams (e.g., Salmon and Clearwater Rivers) of the southern PNW domain also show lower projected flows (Figures 6 and 9). The estimated stream temperature sensitivity to air temperature and streamflow changes indicates that air temperature alone is a poor surrogate for determining climate change impacts on aquatic systems, and that more detailed streamflow and energy budget characteristics of various hydroclimate regimes should be considered.

[44] Stream mouths show relatively larger projected changes in mean annual temperatures than in mean summer temperatures (Table 3) because most PNW streams reflect

Table 2. Model-Estimated Mean Annual and Summer Stream Flow Changes Projected for the 2020s, 2040s, and 2080s Across the PNW Domains, Compared to the 1980s (1970–1999)[a]

Domains	Mean ($m^3 s^{-1}$)	Range ($m^3 s^{-1}$)	Mean (%)	Range (%)	N_1	N_2
			Mean Annual Stream Flow Change by 2020s			
Snow dominant	−9.1	−157.4– 24.1	−4.2	−19.5–7.9	547	2553
Transient	−3.3	−222.6–4.7	−2.7	−16.2–21.2	613	2121
Rain dominant	−4.0	−51.8–1.4	−3.3	−9.4–5.0	57	395
River mouths	−6.5	−222.6–1.4	−2.1	−10.0–5.0	10	37
PNW	−6.2	−222.6–24.1	−3.5	−19.5–21.2	1217	5069
			Mean Annual Stream Flow Change by 2040s			
Snow dominant	10.4	−37.4–182.6	0.3	−19.6–13.6	1645	1455
Transient	0.3	−37.5–115.5	0.9	−14.5–36.7	1566	1168
Rain dominant	−1.7	−34.3–7.2	0.1	−6.3–9.8	205	247
River mouths	3.8	−6.3–115.3	1.7	−9.5–9.8	34	13
PNW	5.1	−37.5–182.6	0.6	−19.6–36.7	3416	2870
			Mean Annual Stream Flow Change by 2080s			
Snow dominant	34.8	−10.7–510.3	6.5	−20.4–20.0	2774	326
Transient	4.2	−19.0–472.3	4.6	−12.5–51.0	2303	431
Rain dominant	−0.2	−38.1–21.8	3.7	−7.3–17.1	321	131
River mouths	15.1	−6.2–472.1	6.2	−9.4–16.7	44	3
PNW	19.0	−38.1–510.3	5.5	−20.4–51.0	5398	888
			Mean Summer Stream Flow Change by 2020s			
Snow dominant	−84	−1185.9–0.0	−23.1	−65.1 to −0.5	1	3099
Transient	−11.4	−1289.7–0.8	−15.2	−60.2–21.1	184	2550
Rain dominant	−5	−63.8–0.0	−18.6	−42.8 to −3.8	1	451
River mouths	−33.7	−1289.7–0.0	−16.2	−35.8 to −0.3	0	47
PNW	−46.8	−1289.7–0.8	−19.3	−65.1–21.1	186	6100
			Mean Summer Stream Flow Change by 2040s			
Snow dominant	−107.1	−1511.0–0.2	−29.0	−74.5–4.5	21	3079
Transient	−14.4	−1646.5–1.8	−18.4	−79.4–34.5	305	2429
Rain dominant	−6.4	−82.3–0.0	−22.4	−57.2 to −4.5	1	451
River mouths	−43.3	−1646.5–0.3	−20.6	−49.7–2.3	1	46
PNW	−59.5	−1646.5–1.8	−23.9	−79.4–34.5	327	5959
			Mean Summer Stream Flow Change by 2080s			
Snow dominant	−148.7	−2228.9–0.4	−37.8	−85.3–10.2	42	3058
Transient	−18.6	−2061.8–2.6	−22.2	−90.8–44.8	407	2327
Rain dominant	−7.8	−100.9–0.0	−27.6	−70.1 to −6.0	1	451
River mouths	−58	−2228.9–0.6	−26.2	−63.3–4.6	4	43
PNW	−82	−2228.9–2.6	−30.3	−90.8–44.8	450	5836

[a]N_1 and N_2 are the number of grid cells showing positive and negative trends in estimated flow changes. Only river mouth cells with upstream drainage areas exceeding 300 km^2 (five 1/16 degree grid cells) are represented.

rain dominant regimes. However, the Columbia is the largest PNW stream and represents a snow dominant system; the Columbia River mouth shows the largest projected summer temperature change among all other PNW streams, increasing from 1.88°C (2020s) to 4.37°C (2080s).

7. Summary and Conclusions

[45] A new coupled streamflow and temperature model (DRTT) was developed, by combining stream thermal dynamics simulations with a source-sink routing model. The DRTT model has three desirable characteristics, including (1) spatially distributed and continuous daily streamflow and temperature estimates for larger domains consistent with macroscale hydrology model based runoff simulations, (2) process based representation of daily streamflow and temperature conditions along entire streamflow paths, and (3) relatively simple model setup and calibration. In this study the DRTT model was applied with VIC runoff simulations to assess regional patterns, temporal variability and potential climate change impacts on daily streamflow and temperature conditions for PNW streams. The VIC model was used to provide gridded runoff and other forcing variables for the DRTT simulations. We used the same historical and climate change projected inputs for the VIC model as *Elsner et al.* [2010], with additional VIC model calibrations to achieve more refined runoff and streamflow simulations for selected subbasins. Model validation and sensitivity analyses indicated that stream temperature simulation accuracy is strongly dependent on the accuracy of the streamflow simulations, while the DRTT simulations showed generally favorable correspondence with stream gauge historical flow and temperature measurement records at 14 locations and 12 streams across the PNW domain.

[46] The VIC model driven DRTT simulations were then used to assess potential PNW streamflow and temperature impacts from projected future (to 2100) climate conditions represented by an ensemble of 20 GCMs (A1B scenario)

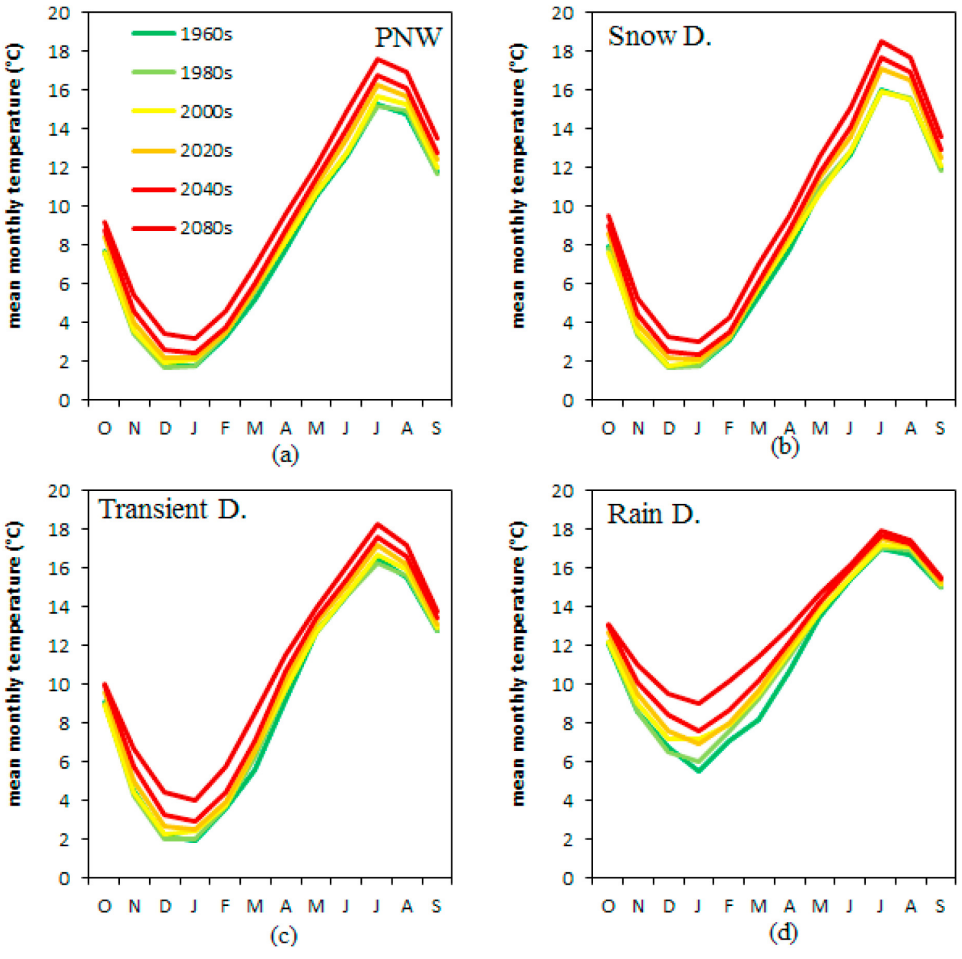

Figure 11. Same as Figure 8, but for the stream temperature.

from the IPCC AR4 assessment. The model results indicate that regional streamflow and temperature conditions are strongly sensitive to projected near term climate change. The entire PNW shows a relatively small projected decrease (−3.5%) in mean annual streamflow in the 2020s, and projected 0.6% (2040s) and 5.5% (2080s) flow increases in later years relative to historical (1980s) conditions. The corresponding temperature simulations indicate projected mean annual stream temperature increases from 0.55°C (2020s) to 1.68°C (2080s) relative to the 1980s. However, larger changes are projected for summer streamflow and temperature conditions. The mean summer streamflow is projected to decrease from 19.3% (2020s) to 30.3% (2080s), with increasing summer stream temperatures from 0.92°C (2020s) to 2.10°C (2080s) for the same period. The warming climate is projected to have more significant impacts on snow dominant streams, especially in the summer season, with relatively larger changes compared to streams in transient and rain dominant regime areas. Snow dominant streams show the largest summer streamflow decreases, ranging from 23.1% (2020s) to 37.8% (2080s), and the highest stream temperature increases (from 1.23°C to 2.74°C for the same period). Significant seasonal shifts in streamflow (toward earlier streamflow peaks) for streams in snow dominant regimes and decreases in peak flows for streams in transient regimes are projected for the mid and far future scenarios, though there is no significant seasonal temperature shift projected in stream temperatures for streams in these areas.

[47] The projected changes in streamflow and temperature patterns and seasonal characteristics will likely have major impacts on aquatic ecosystems and may reshape the patterns of freshwater salmon habitat and associated productivity in PNW rivers. Most importantly, projected decreases in summer streamflow and associated increases in stream temperatures suggests a future with increasing summertime thermal stress, a major bottleneck for cold water fish in the PNW. The flow and temperature simulations documented in this paper are being used in more detailed studies of PNW salmon habitat distributions and potential vulnerability [*Beechie et al.*, 2012; *Whited et al.*, 2012]. Together with the results in this study, *Whited et al.* [2012] developed a river scape analysis and decision support system to address the need for a comprehensive database to describe and compare North Pacific Rim basins on the basis of their freshwater habitat abundance, relative complexity and potential vulnerability; *Beechie et al.* [2012] suggests the change in streamflow and temperature may have significant impacts on PNW salmon populations and the food webs that support them,

Table 3. Model-Projected Mean Annual and Summer Stream Temperature and Air Temperature Changes for the 2020s, 2040s, and 2080s Across PNW Domains, Compared to the 1980s (1970–1999)[a]

	Change (°C)				
	Snow Dominant	Transient	Rain Dominant	River Mouth	PNW
			Mean Annual Stream Temperature Change		
By 2020s					
Mean	0.56	0.54	0.55	0.53	0.55
Range	0.01–1.09	0.01–0.99	0.27–1.03	0.33–0.97	0.01–1.09
By 2040s					
Mean	0.91	0.94	0.93	0.92	0.93
Range	0.03–1.72	0.14–1.72	0.43–1.80	0.58–1.35	0.03–1.80
By 2080s					
Mean	1.63	1.76	1.58	1.62	1.68
Range	0.08–2.98	0.55–3.17	0.80–3.08	1.00–2.31	0.08–3.17
			Mean Summer Stream Temperature Change		
By 2020s					
Mean	1.23	0.66	0.40	0.42	0.92
Range	0.20–2.44	−0.27–2.54	−0.04–2.66	−0.03–1.88	−0.27–2.66
By 2040s					
Mean	1.82	1.01	0.50	0.62	1.37
Range	0.30–3.44	−0.47–3.97	−0.05–4.08	−0.03–2.72	−0.47–4.08
By 2080s					
Mean	2.74	1.62	0.64	0.99	2.10
Range	0.69–4.68	−0.46–5.81	−0.10–5.71	−0.04–4.37	−0.46–5.81
			Mean Annual Air Temperature Change		
By 2020s					
Mean	1.14	1.20	1.26	1.23	1.18
Range	0.90–1.44	0.88–1.43	0.91–1.40	1.10–1.40	0.88–1.44
By 2040s					
Mean	2.02	2.12	2.22	2.16	2.08
Range	1.00–2.54	1.58–2.54	1.67–2.44	1.97–2.46	1.00–2.54
By 2080s					
Mean	3.18	3.37	3.46	3.40	3.28
Range	1.00–4.50	2.96–4.50	3.08–4.33	3.59–4.39	1.00–4.50
			Mean Summer Air Temperature Change		
By 2020s					
Mean	1.51	1.58	1.69	1.65	1.56
Range	1.00–1.75	1.13–1.77	1.15–1.76	1.41–1.74	1.00–1.77
By 2040s					
Mean	2.76	2.81	2.98	2.96	2.81
Range	1.00–3.08	2.12–3.06	2.22–3.07	2.76–3.07	1.00–3.08
By 2080s					
Mean	4.46	4.51	4.77	4.79	4.55
Range	1.00–5.48	3.92–5.44	4.02–5.46	5.01–5.45	1.00–5.48

[a]Only river mouth cells with upstream drainage areas exceeding 300 km^2 (five 1/16 degree grid cells) are represented.

while most restoration actions focused on in-stream rehabilitation are unlikely to ameliorate climate change effects.

Notation

q streamflow rate (m^3 s^{-1}).
c kinematic wave celerity (m s^{-1}).
d longitudinal dispersion coefficient (m^2 s^{-1}).
t time (s).
x flow distance (m).
T_w water temperature (°C).
ΔH net heat change rate (W m^{-2}).
f_A effective water pulse surface area exposed to the air (m^2).
C_p specific heat of water (J kg^{-1} °C^{-1}).
M mass of the water pulse (kg).
$\mu_i(t)$ response function at source cell i and time t (s^{-1}).
T_i average lag time (s).
$\prod_i$ representative Péclet number for a flow path (dimensionless).
v_i mean flow velocity for a grid cell (m s^{-1}).
l_i flow distance of for a grid cell (m).
$Q(x,t)$ routed runoff contributed by an upstream source cell (m^3).
$R(x,s)$ runoff generated in the source cell (m^3).
$T_{w,n}(x,t)$ stream temperature of the target cell at location x and time t when n upstream water pulses have reached and mixed (°C).
$Q_{n-1}(x,t)$ streamflow of the target cell when *n-1* water pulses have reached and mixed (m^3).
$T_{w,n-1}(x,t)$ stream temperature of the target cell when $n-1$ water pulses have reached and mixed (°C).
$T_w(x,t)$ temperature of the nth water pulse when it reaches the target cell at time t (°C).

Q_p magnitude of a water pulse (m^3).
α linear coefficient that define the shape of f_A response to Q_p (dimensionless).
β exponent that define the shape of f_A response to Q_p (dimensionless).
L upstream dominant stream length (m).
$\bar{l}$ average flow distance of each grid cell from all upstream grid cells (m).
$T_{headwater}$ headwater temperature (°C).
T_{annual} mean annual air temperature (°C).
T_{air} actual air temperature (°C).
H_s net solar short-wave radiation (W m^{-2}).
H_l net long-wave radiation (W m^{-2}).
H_e flux of latent heat (W m^{-2}).
H_c conductive heat flux at the streambed (W m^{-2}).
H_h flux of sensible heat (W m^{-2}).
H_a advective heat flux (W m^{-2}).
H_{si} incoming short-wave solar radiation (W m^{-2}).
H_{li} incoming atmosphere long-wave radiation (W m^{-2}).
σ Stefan-Boltzmann constant (5.67×10^{-8} W m^{-2} K^{-4}).
ρ water density (kg m^{-3}).
E evaporation rate (mm d^{-1}).
Le latent heat of vaporization (J/kg).
K_l empirical coefficient for the turbulent exchange of water vapor (mm/(d hPa)).
e_{sat} saturation vapor pressure at the water surface (hPa).
e actual vapor pressure (hPa).
V_{wind} estimated local wind speed at 10m height (m s^{-1}).
F_{wind} dimensionless factor for wind sheltering by riparian vegetation (dimensionless).
γ psychrometric constant at normal pressure (0.655 hPa/°C).
P actual air pressure (hPa).

[48] **Acknowledgments.** This work was conducted at the University of Montana (UMT) with financial support from the Gordon and Betty Moore Foundation. The authors would like to thank Wilfred Wollheim and the two anonymous reviewers for their very constructive comments and suggestions for improving the paper. The authors would also like to thank John Lucotch and Niels Maumenee for assistance in data processing.

References

Anderson, E. R. (1954), Energy-budget studies, water-loss investigation: Lake Hefner studies, *U.S. Geol. Surv. Prof. Pap.*, *269*, 71–119.

Beechie, T., et al. (2012), Restoring salmon in a changing climate, *River Res. Appl.*, doi:10.1002/rra.2590, in press.

Bogan, T., O. Mohseni, and H. G. Stefan (2003), Stream temperature-equilibrium temperature relationship, *Water Resour. Res.*, *39*(9), 1245, doi:10.1029/2003WR002034.

Bogan, T., H. G. Stefan, and O. Mohseni (2004), Imprints of secondary heat sources on the stream temperature/equilibrium temperature relationship, *Water Resour. Res.*, *40*, W12510, doi:10.1029/2003WR002733.

Bras, R. A. (1990), *Hydrology: An Introduction to Hydrologic Science*, 643 pp., Addison-Wesley, Boston, Mass.

Brown, L. E., and D. M. Hannah (2008), Spatial heterogeneity of water temperature across an alpine river basin, *Hydrol. Processes*, *22*, 954–967, doi:10.1002/hyp.

Caissie, D., M. G. Satish, and N. El-Jabi (2007), Predicting water temperatures using a deterministic model: Application on Miramichi River catchments (New Brunswick, Canada), *J. Hydrol.*, *336*(3), 303–315.

Chow, V. T., D. R. Maidment, and L. W. Mays (1988), *Applied Hydrology*, McGraw-Hill, New York.

Christensen, N., and D. P. Lettenmaier (2007), A multimodel ensemble approach to assessment of climate change impacts on the hydrology and water resources of the Colorado River basin, *Hydrol. Earth Syst. Sci.*, *11*, 1417–1434.

Constantz, J. (1998), Interaction between stream temperature, streamflow, and groundwater exchanges in alpine streams, *Water Resour. Res.*, *34*(7), 1609–1615.

Duan, Q., S. Sorooshian, and V. Gupta (1992), Effective and efficient global optimization for conceptual rainfall-runoff models, *Water Resour. Res.*, *28*(4), 1015–1031, doi:10.1029/91WR02985.

Duan, Q., S. Sorooshian, and V. K. Gupta (1994), Optimal use of the SCE-UA global optimization method for calibrating watershed models, *J. Hydrol.*, *158*, 265–284.

Ducharne, A. (2007), Importance of stream temperature to climate change impact on water quality, *Hydrol. Earth Syst. Sci. Discuss.*, *4*, 2425–2460.

Dunham, J., B. Rieman, and G. Chandler (2003), Influences of temperature and environmental variables on the distribution of bull trout within streams at the southern margin of its range, *North Am. J. Fish. Manage.*, *23*, 894–904.

Elsner, M. M., L. Cuo, N. Voisin, J. Deems, A. F. Hamlet, J. A. Vano, K. E. B. Mickelson, S. Y. Lee, and D. P. Lettenmaier (2010), Implications of 21st century climate change for the hydrology of Washington state, *Clim. Change*, *102*(1–2), 225–260, doi:10.1007/s10584-010-9855-0.

Gu, R. R., and Y. Li (2002), River temperature sensitivity to hydraulic and meteorological parameters, *J. Environ. Manage.*, *66*(1), 43–56.

Haag, I., and A. Luce (2008), The integrated water balance and water temperature model LARSIM-WT, *Hydrol. Processes*, *22*(7), 1046–1056.

Hamlet, A. F., and D. P. Lettenmaier (1999), Effects of climate change on hydrology and water resources of the Columbia River basin, *J. Am. Water. Resour. Assoc.*, *35*, 1597–1624.

Hamlet, A. F., and D. P. Lettenmaier (2000), Long-range climate forecasting and its use for water management in the Pacific Northwest region of North America, *J. Hydroinf.*, *2*(3), 163–182.

Hamlet, A. F., and D. P. Lettenmaier (2005), Production of temporally consistent gridded precipitation and temperature fields for the continental United States, *J. Hydrometeorol.*, *6*, 330–336.

Hamlet, A. F., and D. P. Lettenmaier (2007), Effects of 20th century warming and climate variability on flood risk in the western U.S., *Water Resour. Res.*, *43*, W06427, doi:10.1029/2006WR005099.

Hamlet, A. F., et al. (2010a), Final project report for the Columbia Basin Climate Change Scenarios Project, Clim. Impacts Group, Univ. of Wash., Seattle. [Available at http://www.hydro.washington.edu/2860/report/.]

Hamlet, A. F., S. Y. Lee, K. E. B. Mickleson, and M. M. Elsner (2010b), Effects of projected climate change on energy supply and demand in the Pacific Northwest and Washington State, *Clim. Change*, *102*, 103–128, doi:10.1007/s10584-010-9857-y.

Hebert, C., D. Caissie, M. G. Satish, and N. El-Jabi (2011), Study of stream temperature dynamics and corresponding heat fluxes within Miramichi River catchments (New Brunswick, Canada), *Hydrol. Processes*, *25*(15), 2439–2455, doi:10.1002/hyp.8021.

Intergovernmental Panel on Climate Change (2000), *Special Report on Emissions Scenarios: A Special Report of Working Group III of the Intergovernmental Panel on Climate Change*, edited by N. Nakićenović and R. Swart, 599 pp., Cambridge Univ. Press, Cambridge, U. K.

Isaak, D., et al. (2010), Effects of climate change and wildfire on stream temperatures and salmonid thermal habitat in a mountain river network, *Ecol. Appl.*, *20*(5), 1350–1371.

Johnson, S. L. (2003), Stream temperature: Scaling of observations and issues for modelling, *Hydrol. Processes*, *17*, 497–499.

Kalnay, E., et al. (1996), The NCEP/NCAR 40-year reanalysis project, *Bull. Am. Meteorol. Soc.*, *77*, 437–471.

Kimball, J. S., S. W. Running, and R. R. Nemani (1997), An improved method for estimating surface humidity from daily minimum temperature, *Agric. For. Meteorol.*, *85*, 87–98.

LeBlanc, R. T., R. D. Brown, and J. E. FitzGibbon (1997), Modeling the effects of land use change on the water temperature in unregulated urban streams, *J. Environ. Manage.*, *49*, 445–469.

Liang, X., D. P. Lettenmaier, E. F. Wood, and S. J. Burges (1994), A simple hydrologically based model of land surface water and energy fluxes for GSMs, *J. Geophys. Res.*, *99*(D7), 14,415–14,428.

Liang, X., E. F. Wood, and D. P. Lettenmaier (1996), Surface soil moisture parameterization of the VIC-2L model: Evaluation and modifications, *Global Planet. Change*, *13*, 195–206.

Loáiciga, H. A., D. R. Maidment, and J. B. Valdes (2000), Climate-change impacts in a regional karst aquifer, Texas, USA, *J. Hydrol.*, *227*, 173–194.

Maidment, D. R., F. Olivera, A. Calver, A. Eatherall, and W. Fraczek (1996), Unit hydrograph derived from a spatially distributed velocity field, *Hydrol. Processes*, *10*, 831–844.

Mantua, N., I. Tolver, and A. Hamlet (2010), Climate change impacts on streamflow extremes and summertime stream temperature and their possible consequences for freshwater salmon habitat in Washington state, *Clim. Change*, *102*, 187–223, doi:10.1007/s10584-010-9845-2.

Marsh, P., and T. D. Prowse (1987), Water temperature and heat flux at the base of river ice covers, *Cold Reg. Sci. Technol.*, *14*, 33–50.

Maurer, E. P. (2007), Uncertainty in hydrologic impacts of climate change in the Sierra Nevada, California under two emissions scenarios, *Clim. Change*, *82*(3–4), 309–325.

Maurer, E. P., A. W. Wood, J. C. Adam, D. P. Lettenmaier, and B. Nijssen (2002), A long-term hydrologically based dataset of land surface fluxes and states for the conterminous United States, *J. Clim.*, *15*, 3237–3251.

McCullough, D. A., et al. (2009), Research in thermal biology: Burning questions for coldwater stream fishes, *Rev. Fish. Sci.*, *17*(1), 90–115.

Mohseni, O., and H. G. Stefan (1999), Stream temperature air temperature relationship: A physical interpretation, *J. Hydrol.*, *218*(3–4), 128–141.

Mohseni, O., H. G. Stefan, and T. R. Erickson (1998), A nonlinear regression model for weekly stream temperatures, *Water Resour. Res.*, *34*(10), 2685–2692, doi:10.1029/98WR01877.

Morrison, J., M. C. Quick, and M. G. G. Foreman (2002), Climate change in the Fraser River watershed: Flow and temperature projections, *J. Hydrol.*, *263*, 230–244.

Mote, P. W., and E. P. Salathé Jr. (2010), Future climate in the Pacific Northwest, *Clim. Change*, *102*, 29–50, doi:10.1007/s10584-010-9848-z.

Nash, J. E., and J. V. Sutcliffe (1970), River flow forecasting through conceptual models part I—A discussion of principles, *J. Hydrol.*, *10*(3), 282–290.

Olivera, F., and D. Maidment (1999), Geographic Information Systems (GIS)-based spatially distributed model for runoff routing, *Water Resour. Res.*, *35*(4), 1155–1164, doi:10.1029/1998WR900104.

Olivera, F., J. Famiglietti, and K. Asante (2000), Global-scale flow routing using a source-to-sink algorithm, *Water Resour. Res.*, *36*(8), 2197–2207, doi:10.1029/2000WR900113.

Poff, N. L., and J. V. Ward (1989), Implications of streamflow variability and predictability for lotic community structure: A regional analysis of streamflow patterns, *Can. J. Fish. Aquat. Sci.*, *46*(10), 1805–1818.

Poole, G. C., and C. H. Berman (2001), An ecological perspective on in-stream temperature: Natural heat dynamics and mechanisms of human-caused thermal degradation, *Environ. Manage.*, *27*(6), 787–802, doi:10.1007/s002670010188.

Randall, D. A., et al. (2007), Climate models and their evaluation, in *Climate Change 2007: The Physical Science Basis. Contribution of Working Group I to the Fourth Assessment Report of the Intergovernmental Panel on Climate Change*, edited by S. Solomon et al., Cambridge Univ. Press, Cambridge, U. K.

Risley, J. C., J. Constantz, H. Essaid, and S. Rounds (2010), Effects of upstream dams versus groundwater pumping on stream temperature under varying climate conditions, *Water Resour. Res.*, *46*, W06517, doi:10.1029/2009WR008587.

Sinokrot, B. A., and H. G. Stefan (1993), Stream temperature dynamics: Measurements and modeling, *Water Resour. Res.*, *29*, 2299–2312.

Sullivan, A. B., and S. A. Rounds (2004), Modeling streamflow and water temperature in the North Santiam and Santiam rivers, Oregon, 2001–02, *U.S. Geol. Surv. Sci. Invest. Rep.*, *2004-5001*, 35 pp.

Sullivan, K., D. J. Martin, R. D. Carwell, J. E. Toll, and S. Duke (2000), An analysis of the effects of temperature on salmonids of the Pacific Northwest with implications for selecting temperature criteria, report, Sustainable Ecosyst. Inst., Portland, Oreg.

Tague, C., M. Farrell, G. Grant, S. Lewis, and S. Rey (2007), Hydrogeologic controls on summer stream temperatures in the McKenzie River basin, Oregon, *Hydrol. Processes*, *21*(24), 3288–3300.

Thornton, P. E., and S. W. Running (1999), An improved algorithm for estimating incident daily solar radiation from measurements of temperature, humidity, and precipitation, *Agric. For. Meteorol.*, *93*, 211–228.

van Vliet, M. T. H., F. Ludwig, J. J. G. Zwolsman, G. P. Weedon, and P. Kabat (2011), Global river temperatures and sensitivity to atmospheric warming and changes in river flow, *Water Resour. Res.*, *47*, W02544, doi:10.1029/2010WR009198.

Webb, B. W., and Y. Zhang (1997), Spatial and seasonal variability in the components of the river heat budget, *Hydrol. Processes*, *11*, 79–101.

Webb, B. W., D. M. Hannah, R. D. Moore, L. E. Brown, and F. Nobilis (2008), Recent advances in stream and river temperature research, *Hydrol. Processes*, *22*(7), 902–918.

Wenger, S. J., et al. (2011), Flow regime, temperature, and biotic interactions drive differential declines of trout species under climate change, *Proc. Natl. Acad. Sci. U. S. A.*, *108*(34), 14,175–14,180, doi:10.1073/pnas.1103097108.

Whited, D. C., J. S. Kimball, J. A. Lucotch, N. K. Maumenee, H. Wu, S. D. Chilcote, and J. A. Stanford (2012), A riverscape analysis tool developed to assist wild salmon conservation across the north Pacific Rim, *Fisheries*, *37*(7), 305–314.

Wu, H., J. S. Kimball, N. Mantua, and J. Stanford (2011), Automated upscaling of river networks for macroscale hydrological modeling, *Water Resour. Res.*, *47*, W03517, doi:10.1029/2009WR008871.

Yang, D., B. Liu, and B. Ye (2005), Stream temperature changes over Lena River basin in Siberia, *Geophys. Res. Lett.*, *32*, L05401, doi:10.1029/2004GL021568.

Yearsley, J. R. (2009), A semi-Lagrangian water temperature model for advection-dominated river systems, *Water Resour. Res.*, *45*, W12405, doi:10.1029/2008WR007629.